

## Supporting Information to: Anion and Ether Group Influence in Protic Guanidinium Ionic Liquids

Daniel Rauber,<sup>a</sup> Frederik Philippi,<sup>b</sup> Julian Becker,<sup>b</sup> Josef Zapp,<sup>c</sup> Bernd Morgenstern,<sup>a</sup> Björn Kuttich,<sup>b</sup> Tobias Kraus,<sup>a, d</sup> Rolf Hempelmann,<sup>a</sup> Patricia Hunt,<sup>b, e</sup> Tom Welton,<sup>b</sup> and Christopher W.M. Kay<sup>a, f</sup>

<sup>a</sup> Department of Chemistry, Saarland University, Campus B 2.2, 66123 Saarbrücken, Germany;  
E-mail: daniel.rauber@uni-saarland.de

<sup>b</sup> Molecular Sciences Research Hub, Imperial College London, White City Campus, London W12 0BZ, United Kingdom

<sup>c</sup> Pharmaceutical Biology, Saarland University, Campus B 2 3, 66123 Saarbrücken, Germany

<sup>d</sup> INM-Leibniz Institute for New Materials, Campus D2 2, 66123 Saarbrücken, Germany

<sup>e</sup> School of Chemical and Physical Sciences, Victoria University of Wellington, New Zealand

<sup>f</sup> London Centre for Nanotechnology, University College London, 17-19 Gordon Street, London WC1H 0AH, UK; E-mail: c.kay@ucl.ac.uk

# Contents

<b>S1</b>	<b>Synthesis of the Ionic Liquids and Precursors</b>	<b>3</b>
S1.1	Synthesis of the Precursors . . . . .	3
S1.1.1	Synthesis of 2-(2-ethoxyethyl)-1,1,3,3-tetramethyl guanidine . . . . .	3
S1.1.2	Synthesis of 2-pentyl-1,1,3,3-tetramethyl guanidine . . . . .	4
S1.2	Synthesis of the Protic Ionic Liquids . . . . .	4
S1.2.1	Synthesis of 2-(2-ethoxyethyl)-1,1,3,3-tetramethyl guanidinium bis(fluorosulfonyl)imide [2O2HTMG][FSI ] . . . . .	4
S1.2.2	Synthesis of 2-(2-ethoxyethyl)-1,1,3,3-tetramethyl guanidinium bis(trifluoromethanesulfonyl)imide [2O2HTMG][NTf <sub>2</sub> ] . . . . .	4
S1.2.3	Synthesis of 2-(2-ethoxyethyl)-1,1,3,3-tetramethyl guanidinium bis(pentafluoroethanesulfonyl)imide [2O2HTMG][BETI] . . . . .	5
S1.2.4	Synthesis of 2-(2-ethoxyethyl)-1,1,3,3-tetramethyl guanidinium triflate [2O2H TMG][OTf] . . . . .	5
S1.2.5	Synthesis of 2-(2-ethoxyethyl)-1,1,3,3-tetramethyl guanidinium hexafluorophosphate [2O2H TMG][PF <sub>6</sub> ] . . . . .	6
S1.2.6	Synthesis of 2-(2-ethoxyethyl)-1,1,3,3-tetramethyl guanidinium tetrafluoroborate [2O2H TMG][BF <sub>4</sub> ] . . . . .	6
S1.2.7	Synthesis of 2-(2-ethoxyethyl)-1,1,3,3-tetramethyl guanidinium trifluoroacetate [2O2H TMG][TFA] . . . . .	6
S1.2.8	Synthesis of 2-pentyl-1,1,3,3-tetramethyl guanidinium bis(trifluoromethanesulfonyl)imide [C <sub>5</sub> HTMG][NTf <sub>2</sub> ] . . . . .	7
S1.2.9	Synthesis of 2-pentyl-1,1,3,3-tetramethyl guanidinium hexafluorophosphate [C <sub>5</sub> HTMG][PF <sub>6</sub> ] . . . . .	7
<b>S2</b>	<b>Thermogravimetric Analysis</b>	<b>8</b>
<b>S3</b>	<b>Density</b>	<b>9</b>
<b>S4</b>	<b>Viscosity</b>	<b>11</b>
<b>S5</b>	<b>Specific conductivity</b>	<b>13</b>
<b>S6</b>	<b>Molar Conductivity</b>	<b>15</b>
<b>S7</b>	<b>Walden Relation</b>	<b>17</b>
<b>S8</b>	<b>Small Angle X-ray Scattering</b>	<b>20</b>
<b>S9</b>	<b>Proton Affinity</b>	<b>22</b>
<b>S10</b>	<b>Additional Computations</b>	<b>23</b>

S10.1	Ion Volumes and Radii . . . . .	23
S10.2	H-bonding criteria . . . . .	23
S10.3	Isolated Cations . . . . .	24
S10.3.1	Potential Energy Surfaces . . . . .	24
S10.3.2	[2O1TMG] <sup>+</sup> . . . . .	26
S10.3.3	Electrostatic Potential Histograms . . . . .	28
S10.4	Ion Pairs . . . . .	29
S10.4.1	[2O1HTMG][TFA] . . . . .	29
S10.4.2	[2O1HTMG][NTf <sub>2</sub> ] . . . . .	29
S10.4.3	Proton Scan . . . . .	34
<b>S11</b>	<b>Two-dimensional NMR spectra</b>	<b>35</b>
<b>S12</b>	<b>Crystal data and structure refinement</b>	<b>40</b>
<b>S13</b>	<b>References</b>	<b>54</b>

# S1 Synthesis of the Ionic Liquids and Precursors

Purity and identity of the synthesized ionic liquids was confirmed using multinuclear NMR spectroscopy prior to the physicochemical properties. The guanidinium bases were synthesized as reported below. Lithium salts of the imides, [Li][FSI] (99%), [Li][NTf<sub>2</sub>] (>99%) and [Li][BETI] (99%) were obtained from IoLiTec (Germany) and used without further purification. Trifluoromethane sulfonic acid ( $\geq$ 99%), hexafluorophosphoric acid ( $\sim$ 55 wt.% in H<sub>2</sub>O), tetrafluoroboric acid (48 wt.% in H<sub>2</sub>O), trifluoroacetic acid (99%) and triethylamine (99%) were purchased from Sigma Aldrich (USA) and used as obtained. 2-ethoxyethylamine (98%) and pentylamine (>98%) from TCI Germany were purified by distillation. NMR spectra were recorded on an AVANCE II 400 NMR spectrometer (Bruker, USA) using the residual solvent signal as reference. Chemical shifts  $\delta$  are given in ppm vs. Si(CH<sub>3</sub>)<sub>4</sub> (for <sup>1</sup>H and <sup>13</sup>C NMR) or CFCl<sub>3</sub> (for <sup>19</sup>F NMR)

## S1.1 Synthesis of the Precursors

The chloro-N,N,N',N'-tetramethylformamidinium chloride used for the preparation of the guanidines was synthesized as previously<sup>1</sup> reported using a modified literature protocol.<sup>2</sup> Synthesis of the guanidines was conducted under argon atmosphere due to the sensitivity of the chloride towards ambient moisture similar to literature preparations of other 2-(alkyl)-1,1,3,3-tetramethyl guanidines.<sup>1-3</sup>

### S1.1.1 Synthesis of 2-(2-ethoxyethyl)-1,1,3,3-tetramethyl guanidine

The free guanidine base was synthesized from chloro-N,N,N',N'-tetramethylformamidinium chloride (1.0 eq.) that was dissolved in dry acetonitrile under argon atmosphere and cooled to 0 °C by an ice bath. To the solution 2.1 eq. of 2-ethoxyethylamine were added dropwise for 3 hours. After completion of the addition the reaction mixture was stirred for 4 hours while allowing to warm to ambient temperature. The solvent and excess of amine were removed by rotary evaporation obtaining a highly viscous residue. To this residue 30 wt.% aqueous NaOH-solution was added, followed by stirring of the resulting biphasic system for 40 min. The organic phase was extracted three times with diethyl ether, the ethereal phase dried with MgSO<sub>4</sub>, filtered and the solvent removed on a rotary evaporator. The residue was subjected to fractional vacuum distillation to obtain the free guanidine base (b.p. of 78 °C at 3.0 mbar) as a colorless liquid in 52% yield.

<sup>1</sup>H-NMR (400 MHz, DMSO-d<sub>6</sub>):  $\delta$  / ppm = 3.60 – 3.42 (m, 4H, CH<sub>2</sub>-CH<sub>3</sub> + N-CH<sub>2</sub>), 3.29 (t, 2H, N-CH<sub>2</sub>-CH<sub>2</sub>), 2.71 (s, 6H, N(CH<sub>3</sub>)<sub>2</sub>), 2.61 (s, 6H, N(CH<sub>3</sub>)<sub>2</sub>), 1.17 (t, *J* = 7.0 Hz, 3H, CH<sub>2</sub>-CH<sub>3</sub>).

<sup>13</sup>C{<sup>1</sup>H}-NMR (101 MHz, DMSO-d<sub>6</sub>):  $\delta$  / ppm = 161.06 (s, CN<sub>3</sub>), 72.78 (s, N-CH<sub>2</sub>-CH<sub>2</sub>), 66.44 (s, CH<sub>2</sub>-CH<sub>3</sub>), 49.64 (s, N-CH<sub>2</sub>), 39.69 (s, N(CH<sub>3</sub>)<sub>2</sub>), 38.91 (s, N(CH<sub>3</sub>)<sub>2</sub>), 15.37 (s, CH<sub>2</sub>-CH<sub>3</sub>).

### S1.1.2 Synthesis of 2-pentyl-1,1,3,3-tetramethyl guanidine

The title compound was synthesized in similar way to 2-(2-ethoxyethyl)-1,1,3,3-tetramethyl guanidine using 1-pentylamine instead of 2-ethoxyethylamine. The product was isolated in 55% as colorless yield by fractional vacuum distillation (b.p. of 85 °C at 3.3 mbar).

**<sup>1</sup>H-NMR** (400 MHz, CDCl<sub>3</sub>):  $\delta$  / ppm = 3.05 (t, *J* = 7.0 Hz, 2H, N-CH<sub>2</sub>), 2.69 (s, 6H, N(CH<sub>3</sub>)<sub>2</sub>), 2.60 (s, 6H, N(CH<sub>3</sub>)<sub>2</sub>), 1.55 – 1.40 (m, 2H, N-CH<sub>2</sub>-CH<sub>2</sub>), 1.33 – 1.15 (m, 4H, N-(CH<sub>2</sub>)<sub>2</sub>-(CH<sub>2</sub>)<sub>2</sub>), 0.85 (t, *J* = 6.6 Hz, 3H, CH<sub>2</sub>-CH<sub>3</sub>).

**<sup>13</sup>C{<sup>1</sup>H}-NMR** (101 MHz, DMSO-d<sub>6</sub>):  $\delta$  / ppm = 160.02 (s, CN<sub>3</sub>), 49.29 (s, N-CH<sub>2</sub>), 39.70 (s, N(CH<sub>2</sub>)<sub>3</sub>), 39.03 (s, N(CH<sub>2</sub>)<sub>3</sub>), 32.33 (s, N-CH<sub>2</sub>-CH<sub>2</sub>), 29.78 (s, N-(CH<sub>2</sub>)<sub>2</sub>-CH<sub>2</sub>), 22.64 (s, N-(CH<sub>2</sub>)<sub>3</sub>-CH<sub>2</sub>), 14.23 (s, CH<sub>2</sub>-CH<sub>3</sub>).

## S1.2 Synthesis of the Protic Ionic Liquids

### S1.2.1 Synthesis of 2-(2-ethoxyethyl)-1,1,3,3-tetramethyl guanidinium bis(fluorosulfonyl)imide [2O2HTMG][FSI]

The ether-substituted protic guanidinium ionic liquids was synthesized by protonation of the free base 2-(2-ethoxyethyl)-1,1,3,3-tetramethyl guanidine dissolved in water with aqueous HCl (1.2 eq.), followed by anion exchange reaction by addition solid lithium bis(fluorosulfonyl)imide to the homogeneous reaction mixture. After the addition of the lithium salt, the resulting biphasic mixture was stirred for 6 hours and extracted with dichloromethane 3 times. The combined organic phases were washed with small amounts of water until the aqueous phase showed a negative AgNO<sub>3</sub> test for halides. Afterwards the organic phase was washed an additional time, dried with MgSO<sub>4</sub>, filtered and the solvent removed by means of rotary evaporation. The obtained residue was dried on a Schlenk line in oil pump vacuum at 50 °C for two days. The product was obtained in 97% yield as slightly yellow liquid.

**<sup>1</sup>H-NMR** (400 MHz, CDCl<sub>3</sub>):  $\delta$  / ppm = 5.77 (t, *J* = 5.72 Hz, 1H, N-H), 3.57 (t, *J* = 4.95 Hz, 2H, N-CH<sub>2</sub>-CH<sub>2</sub>), 3.50 (q, *J* = 7.01 Hz, 2H, CH<sub>2</sub>-CH<sub>3</sub>), 3.35 (td, *J* = 5.55 Hz, *J* = 4.38 Hz, 2H, N-CH<sub>2</sub>), 2.99 (s, 12H, N(CH<sub>3</sub>)<sub>2</sub>), 1.16 (t, *J* = 7.01 Hz, 3H, CH<sub>2</sub>-CH<sub>3</sub>).

**<sup>13</sup>C{<sup>1</sup>H}-NMR** (101 MHz, CDCl<sub>3</sub>):  $\delta$  / ppm = 162.51 (s, CN<sub>3</sub>), 68.50 (s, N-CH<sub>2</sub>-CH<sub>2</sub>), 66.68 (s, CH<sub>2</sub>-CH<sub>3</sub>), 45.22 (s, N-CH<sub>2</sub>), 39.94 (s, N(CH<sub>3</sub>)<sub>2</sub>), 15.15 (s, CH<sub>2</sub>-CH<sub>3</sub>).

**<sup>19</sup>F{<sup>1</sup>H}-NMR** (377 MHz, CDCl<sub>3</sub>):  $\delta$  / ppm = 52.57 (s).

### S1.2.2 Synthesis of 2-(2-ethoxyethyl)-1,1,3,3-tetramethyl guanidinium bis(trifluoromethanesulfonyl)imide [2O2HTMG][NTf<sub>2</sub>]

The title compound was synthesized in similar manner to [2O2HTMG][FSI] using lithium bis(trifluoromethanesulfonyl)imide as anions source. After drying at 50 °C in high vacuum for two days the product was obtained in 97% yield as colorless liquid.

**<sup>1</sup>H-NMR** (400 MHz, CDCl<sub>3</sub>):  $\delta$  / ppm = 5.96 (t,  $J$  = 5.72 Hz, 1H, N-H), 3.55 (t,  $J$  = 4.95 Hz, 2H, N-CH<sub>2</sub>-CH<sub>2</sub>), 3.49 (q,  $J$  = 7.01 Hz, 2H, CH<sub>2</sub>-CH<sub>3</sub>), 3.36 – 3.29 (m, N-CH<sub>2</sub>), 2.98 (s, 12H, N(CH<sub>3</sub>)<sub>2</sub>), 1.15 (t,  $J$  = 7.01 Hz, 3H, CH<sub>2</sub>-CH<sub>3</sub>).

**<sup>13</sup>C{<sup>1</sup>H}-NMR** (101 MHz, CDCl<sub>3</sub>):  $\delta$  / ppm = 162.63 (s, CN<sub>3</sub>), 119.92 (q,  $J$  = 321.25 Hz, CF<sub>3</sub>) 68.50 (s, N-CH<sub>2</sub>-CH<sub>2</sub>), 66.68 (s, CH<sub>2</sub>-CH<sub>3</sub>), 45.22 (s, N-CH<sub>2</sub>), 39.94 (s, N(CH<sub>3</sub>)<sub>2</sub>), 15.15 (s, CH<sub>2</sub>-CH<sub>3</sub>).

**<sup>19</sup>F{<sup>1</sup>H}-NMR** (377 MHz, CDCl<sub>3</sub>):  $\delta$  / ppm = -78.92 (s).

#### S1.2.3 Synthesis of 2-(2-ethoxyethyl)-1,1,3,3-tetramethyl guanidinium bis(pentafluoroethanesulfonyl)imide [2O2HTMG][BETI]

[2O2HTMG][BETI] was synthesized analogous to [2O2HTMG][FSI] using lithium bis(pentafluoroethylsulfonyl)imide as anion source. The final product was obtained after drying in high vacuum at 45 °C for two days in 98% yield as colorless liquids.

**<sup>1</sup>H-NMR** (400 MHz, CDCl<sub>3</sub>):  $\delta$  / ppm = 6.02 (t,  $J$  = 5.78 Hz, 1H, N-H), 3.55 (t,  $J$  = 4.92 Hz, 2H, N-CH<sub>2</sub>-CH<sub>2</sub>), 3.48 (q,  $J$  = 7.00 Hz, 2H, CH<sub>2</sub>-CH<sub>3</sub>), 3.35 (td,  $J$  = 5.58 Hz,  $J$  = 4.38 Hz, 2H, N-CH<sub>2</sub>), 2.97 (s, 12H, N(CH<sub>3</sub>)<sub>2</sub>), 1.14 (t,  $J$  = 7.00 Hz, 3H, CH<sub>2</sub>-CH<sub>3</sub>).

**<sup>13</sup>C{<sup>1</sup>H}-NMR** (101 MHz, CDCl<sub>3</sub>):  $\delta$  / ppm = 162.68 (s, CN<sub>3</sub>), 122.40 – 115.63 (m, CF<sub>3</sub>), 114.84 – 108.37 (m, CF<sub>2</sub>), 68.55 (s, N-CH<sub>2</sub>-CH<sub>2</sub>), 66.63 (s, CH<sub>2</sub>-CH<sub>3</sub>), 45.23 (s, N-CH<sub>2</sub>), 39.86 (s, N(CH<sub>3</sub>)<sub>2</sub>), 15.09 (s, CH<sub>2</sub>-CH<sub>3</sub>).

**<sup>19</sup>F{<sup>1</sup>H}-NMR** (377 MHz, CDCl<sub>3</sub>):  $\delta$  / ppm = -79.01 (s, CF<sub>3</sub>), -117.25 (s, CF<sub>2</sub>).

#### S1.2.4 Synthesis of 2-(2-ethoxyethyl)-1,1,3,3-tetramethyl guanidinium triflate [2O2HTMG][OTf]

To 2-(2-ethoxyethyl)-1,1,3,3-tetramethyl guanidine (1.02 eq.) dissolved in water 1.00 eq. of trifluoromethanesulfonic acid were added dropwise over 30 minutes. The resulting mixture was stirred for two hours and the water removed by rotary evaporation. The residual was dried in high vacuum for two days giving the title protic IL as slightly yellow liquid in 98% yield.

**<sup>1</sup>H-NMR** (400 MHz, CDCl<sub>3</sub>):  $\delta$  / ppm = 6.96 (s, 1H, N-H), 3.58 – 3.53 (m, 2H, N-CH<sub>2</sub>-CH<sub>2</sub>), 3.50 – 3.41 (m, 2H, CH<sub>2</sub>-CH<sub>3</sub>), 3.34 – 3.28 (m, 2H, N-CH<sub>2</sub>), 2.99 (s, 6H, N(CH<sub>3</sub>)<sub>2</sub>), 2.93 (s, 6H, N(CH<sub>3</sub>)<sub>2</sub>), 1.11 (t,  $J$  = 7.81 Hz, 3H, CH<sub>2</sub>-CH<sub>3</sub>).

**<sup>13</sup>C{<sup>1</sup>H}-NMR** (101 MHz, CDCl<sub>3</sub>):  $\delta$  / ppm = 162.84 (s, CN<sub>3</sub>), 120.69 – 115.63 (q,  $J$  = 320.20 Hz, CF<sub>3</sub>), 68.72 (s, N-CH<sub>2</sub>-CH<sub>2</sub>), 66.53 (s, CH<sub>2</sub>-CH<sub>3</sub>), 45.14 (s, N-CH<sub>2</sub>), 39.94 (s, N(CH<sub>3</sub>)<sub>2</sub>), 15.15 (s, CH<sub>2</sub>-CH<sub>3</sub>).

**<sup>19</sup>F{<sup>1</sup>H}-NMR** (377 MHz, CDCl<sub>3</sub>):  $\delta$  / ppm = -79.01 (s).

### S1.2.5 Synthesis of 2-(2-ethoxyethyl)-1,1,3,3-tetramethyl guanidinium hexafluorophosphate [2O2HTMG][PF<sub>6</sub>]

The title compound was synthesized by dropwise addition of 55 wt-% aqueous hexafluorophosphoric acid (1.02 eq.) to a cooled solution of 2-(2-ethoxyethyl)-1,1,3,3-tetramethyl guanidine dissolved in water over 30 minutes. The resulting biphasic mixture was stirred for three hours followed by extraction of the organic phase with dichloromethane for three times. The combined organic extracts were washed with little amount of water several times, dried over MgSO<sub>4</sub>, filtered and subjected to rotary evaporation. The residue was further dried in high vacuum for three days at 35 °C leaving the protic IL as slightly yellow liquid that was obtained in 95% yield.

<sup>1</sup>H-NMR (400 MHz, CDCl<sub>3</sub>):  $\delta$  / ppm = 5.51 (t, *J* = 5.96 Hz, 1H, N-H), 3.57 (t, *J* = 5.01 Hz, 2H, N-CH<sub>2</sub>-CH<sub>2</sub>), 3.49 (q, *J* = 6.98 Hz, 2H, CH<sub>2</sub>-CH<sub>3</sub>), 3.38 – 3.31 (m, 2H, N-CH<sub>2</sub>), 2.99 (s, 12H, N(CH<sub>3</sub>)<sub>2</sub>), 1.15 (t, *J* = 6.97 Hz, 3H, CH<sub>2</sub>-CH<sub>3</sub>).

<sup>13</sup>C{<sup>1</sup>H}-NMR (101 MHz, CDCl<sub>3</sub>):  $\delta$  / ppm = 162.58 (s, CN<sub>3</sub>), 68.55 (s, N-CH<sub>2</sub>-CH<sub>2</sub>), 66.62 (s, CH<sub>2</sub>-CH<sub>3</sub>), 45.20 (s, N-CH<sub>2</sub>), 39.84 (s, N(CH<sub>3</sub>)<sub>2</sub>), 15.17 (s, CH<sub>2</sub>-CH<sub>3</sub>).

<sup>19</sup>F{<sup>1</sup>H}-NMR (377 MHz, CDCl<sub>3</sub>):  $\delta$  / ppm = -72.86 (d, *J* = 711.92 Hz).

<sup>31</sup>P{<sup>1</sup>H}-NMR (162 MHz, CDCl<sub>3</sub>):  $\delta$  / ppm = -144.43 (hept, *J* = 713.06 Hz).

### S1.2.6 Synthesis of 2-(2-ethoxyethyl)-1,1,3,3-tetramethyl guanidinium tetrafluoroborate [2O2HTMG][BF<sub>4</sub>]

2-(2-ethoxyethyl)-1,1,3,3-tetramethyl guanidine (1.05 eq.) was dissolved in water and cooled to 5 °C. To the reaction mixture 1.0 equivalent of 48 wt.-% aqueous tetrafluoroboric acid solution were added dropwise and stirred for four hours. The solvent was removed by rotary evaporation and the excess of guanidine by vacuum distillation. The resulting residue was dried on a Schlenk line for three days giving a colorless liquid in 98% yield.

<sup>1</sup>H-NMR (400 MHz, CDCl<sub>3</sub>):  $\delta$  / ppm = 6.17 (t, *J* = 5.91 Hz, 1H, N-H), 3.57 (t, *J* = 4.96 Hz, 2H, N-CH<sub>2</sub>-CH<sub>2</sub>), 3.47 (q, *J* = 6.99 Hz, 2H, CH<sub>2</sub>-CH<sub>3</sub>), 3.37 – 3.30 (m, 2H, N-CH<sub>2</sub>), 2.98 (s, 12H, N(CH<sub>3</sub>)<sub>2</sub>), 1.13 (t, *J* = 6.98 Hz, 3H, CH<sub>2</sub>-CH<sub>3</sub>).

<sup>11</sup>B-NMR (128 MHz, CDCl<sub>3</sub>):  $\delta$  / ppm = -1.06 (s).

<sup>13</sup>C{<sup>1</sup>H}-NMR (101 MHz, CDCl<sub>3</sub>):  $\delta$  / ppm = 162.82 (s, CN<sub>3</sub>), 68.69 (s, N-CH<sub>2</sub>-CH<sub>2</sub>), 66.55 (s, CH<sub>2</sub>-CH<sub>3</sub>), 45.24 (s, N-CH<sub>2</sub>), 39.84 (s, N(CH<sub>3</sub>)<sub>2</sub>), 15.18 (s, CH<sub>2</sub>-CH<sub>3</sub>).

<sup>19</sup>F{<sup>1</sup>H}-NMR (377 MHz, CDCl<sub>3</sub>):  $\delta$  / ppm = -152.25 (s, <sup>10</sup>BF<sub>4</sub>), -152.30 (s, <sup>11</sup>BF<sub>4</sub>).

### S1.2.7 Synthesis of 2-(2-ethoxyethyl)-1,1,3,3-tetramethyl guanidinium trifluoroacetate [2O2HTMG][TFA]

The title compound was synthesized by dissolving 2-(2-ethoxyethyl)-1,1,3,3-tetramethyl guanidine (1.05 eq.) in water and adding 1.00 eq. of diluted aqueous trifluoroacetic acid. After stirring for 5 hours the solvent was removed by rotary evaporation and dried the

residue dried in high vacuum for two days. The title compound was obtained as colorless liquid in quantitative yield.

**$^1\text{H}$ -NMR** (400 MHz,  $\text{CDCl}_3$ ):  $\delta$  / ppm = 9.47 (s, 1H, N-H), 3.60 (t,  $J$  = 4.93 Hz, 2H, N- $\text{CH}_2$ - $\text{CH}_2$ ), 3.45 (q,  $J$  = 6.99 Hz, 2H,  $\text{CH}_2$ - $\text{CH}_3$ ), 3.32 (t, 2H, N- $\text{CH}_2$ ), 3.01 (s, 6H, N( $\text{CH}_3$ )<sub>2</sub>), 2.88 (s, 6H, N( $\text{CH}_3$ )<sub>2</sub>), 1.10 (t,  $J$  = 7.00 Hz, 3H,  $\text{CH}_2$ - $\text{CH}_3$ ).

**$^{13}\text{C}\{\text{H}\}$ -NMR** (101 MHz,  $\text{CDCl}_3$ ):  $\delta$  / ppm = 163.20 (s, CN<sub>3</sub>), 161.49 (q,  $J$  = 33.19 Hz, CO<sub>2</sub>) 117.28 (q,  $J$  = 295.82 Hz, C<sub>3</sub>), 69.19 (s, N- $\text{CH}_2$ - $\text{CH}_2$ ) 66.54 (s,  $\text{CH}_2$ - $\text{CH}_3$ ), 45.08 (s, N- $\text{CH}_2$ ), 39.92 (s, N( $\text{CH}_3$ )<sub>2</sub>), 15.22 (s,  $\text{CH}_2$ - $\text{CH}_3$ ).

**$^{19}\text{F}\{\text{H}\}$ -NMR** (377 MHz,  $\text{CDCl}_3$ ):  $\delta$  / ppm = -75.28 (s).

#### S1.2.8 Synthesis of 2-pentyl-1,1,3,3-tetramethyl guanidinium bis(trifluoromethanesulfonyl)imide [C<sub>5</sub>HTMG][NTf<sub>2</sub>]

[C<sub>5</sub>HTMG][NTf<sub>2</sub>] was synthesized similar to [2O2HTMG][NTf<sub>2</sub>] using 2-pentyl-1,1,3,3-tetramethyl guanidine as the base. The alkyl-substituted IL was obtained in 98% yield as colorless liquid.

**$^1\text{H}$ -NMR** (400 MHz,  $\text{CDCl}_3$ ):  $\delta$  / ppm = 5.93 (t,  $J$  = 5.52 Hz, 1H, N-H), 3.17 – 3.09 (m, 2H, N- $\text{CH}_2$ ), 2.97 (s, 12H, N( $\text{CH}_3$ )<sub>2</sub>), 1.61 (p,  $J$  = 7.43 Hz, 2H, N- $\text{CH}_2$ - $\text{CH}_2$ ), 1.38 – 1.23 (s, 4H, N-( $\text{CH}_2$ )<sub>2</sub>- $\text{CH}_2$  + N-( $\text{CH}_2$ )<sub>3</sub>- $\text{CH}_2$ ), 0.89 (t,  $J$  = 6.90 Hz, 3H,  $\text{CH}_2$ - $\text{CH}_3$ ).

**$^{13}\text{C}\{\text{H}\}$ -NMR** (101 MHz,  $\text{CDCl}_3$ ):  $\delta$  / ppm = 161.67 (s, CN<sub>3</sub>), 119.92 (q,  $J$  = 321.26 Hz, CF<sub>3</sub>), 45.66 (s, N- $\text{CH}_2$ ) 39.92 (s, N( $\text{CH}_3$ )<sub>2</sub>), 29.59 (s, N- $\text{CH}_2$ - $\text{CH}_2$ ), 28.79 (s, N-( $\text{CH}_2$ )<sub>2</sub>- $\text{CH}_2$ ), 22.24 (s,  $\text{CH}_2$ - $\text{CH}_3$ ), 15.22 (s,  $\text{CH}_2$ - $\text{CH}_3$ ).

**$^{19}\text{F}\{\text{H}\}$ -NMR** (377 MHz,  $\text{CDCl}_3$ ):  $\delta$  / ppm = -78.94 (s).

#### S1.2.9 Synthesis of 2-pentyl-1,1,3,3-tetramethyl guanidinium hexafluorophosphate [C<sub>5</sub>HTMG][PF<sub>6</sub>]

The title compound was synthesized similar to [2O2HTMG][PF<sub>6</sub>] using 2-pentyl-1,1,3,3-tetramethylguanidine instead of the ether-substituted guanidine. The product was obtained in 97% yield as colorless solid.

**$^1\text{H}$ -NMR** (400 MHz,  $\text{CDCl}_3$ ):  $\delta$  / ppm = 5.41 (t,  $J$  = 5.56 Hz, 1H, N-H), 3.15 (dt, 2H,  $J$  = 7.72 Hz,  $J$  = 5.58 Hz, N- $\text{CH}_2$ ), 2.97 (s, 12H, N( $\text{CH}_3$ )<sub>2</sub>), 1.61 (p, 2H,  $J$  = 7.40 Hz, N- $\text{CH}_2$ - $\text{CH}_2$ ), 1.38 – 1.23 (s, 4H, N-( $\text{CH}_2$ )<sub>2</sub>- $\text{CH}_2$  + N-( $\text{CH}_2$ )<sub>3</sub>- $\text{CH}_2$ ), 0.88 (t,  $J$  = 6.81 Hz, 3H,  $\text{CH}_2$ - $\text{CH}_3$ ).

**$^{13}\text{C}\{\text{H}\}$ -NMR** (101 MHz,  $\text{CDCl}_3$ ):  $\delta$  / ppm = 161.66 (s, CN<sub>3</sub>), 45.63 (s, N- $\text{CH}_2$ ) 39.77 (s, N( $\text{CH}_3$ )<sub>2</sub>), 29.51 (s, N- $\text{CH}_2$ - $\text{CH}_2$ ), 28.71 (s, N-( $\text{CH}_2$ )<sub>2</sub>- $\text{CH}_2$ ), 22.23 (s,  $\text{CH}_2$ - $\text{CH}_3$ ), 13.92 (s,  $\text{CH}_2$ - $\text{CH}_3$ ).

**$^{19}\text{F}\{\text{H}\}$ -NMR** (377 MHz,  $\text{CDCl}_3$ ):  $\delta$  / ppm = -72.71 (d,  $J$  = 711.96 Hz).

**$^{31}\text{P}\{\text{H}\}$ -NMR** (162 MHz,  $\text{CDCl}_3$ ):  $\delta$  / ppm = -144.43 (hept,  $J$  = 712.77 Hz).

## S2 Thermogravimetric Analysis

Experimental curves of the thermogravimetric analysis (TGA) are shown in Figure S1. The obtained decomposition temperatures  $T_d$ , obtained as extrapolated onsets, are reported in the main manuscript.

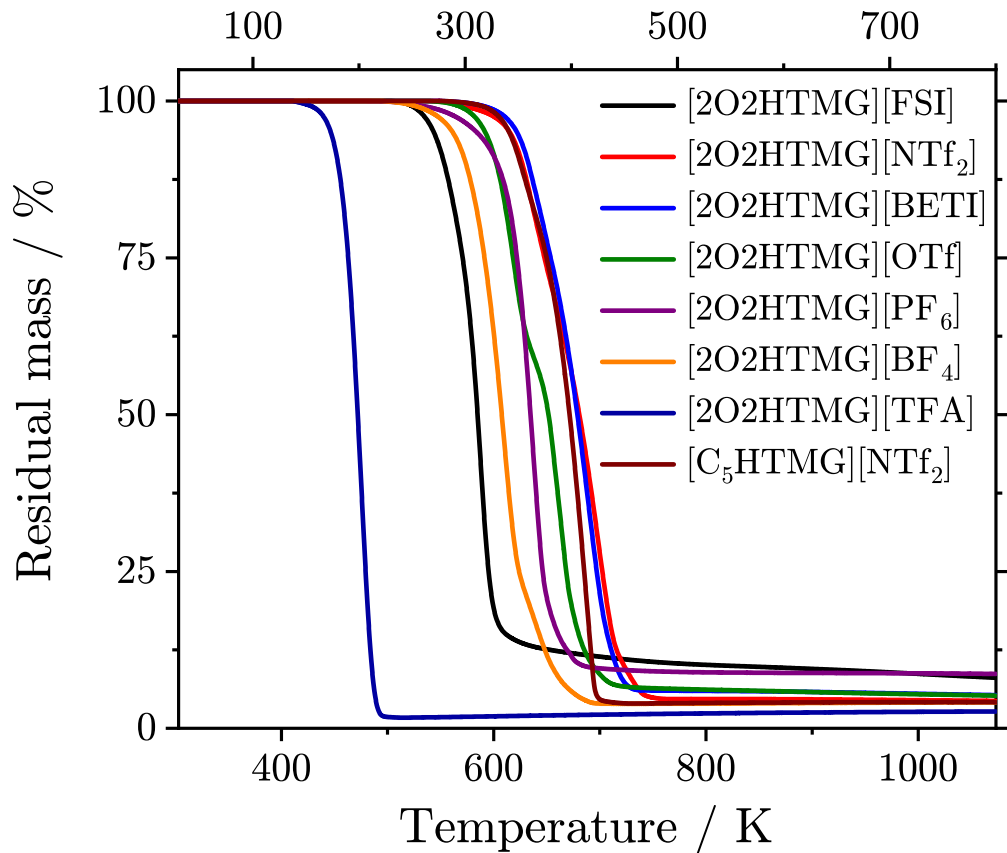


**Figure S1** TGA traces of the investigated guanidinium ionic liquids measured under nitrogen atmosphere with a heating rate of  $+10\text{ }^\circ\text{C min}^{-1}$ .

### S3 Density

Temperature dependent densities  $\rho$  of the investigated guanidinium ionic liquids are given in Table S1 and plotted in Figure S2. Fitting with the linear eqn (S1) yielded the fitting parameters given in Table S2.

$$\rho = a - b \cdot T \quad (\text{S1})$$

**Table S1** Experimental density values of the guanidinium ionic liquids given in  $\text{g} \cdot \text{mL}^{-1}$  at different temperatures.

Ionic liquid	Temperature / $^{\circ}\text{C}$						
	25	35	45	55	65	75	85
[2O2HTMG][FSI]	1.2899	1.2822	1.2740	1.2649	1.2568	1.2484	1.2412
[2O2HTMG][NTf <sub>2</sub> ]	1.3663	1.3576	1.3487	1.3385	1.3287	1.3193	1.3107
[2O2HTMG][BETI]	1.4399	1.4294	1.4184	1.4077	1.3980	1.3870	1.3776
[2O2HTMG][OTf]	1.2415	1.2339	1.2250	1.2169	1.2084	1.2007	1.1941
[2O2HTMG][PF <sub>6</sub> ]	1.2993	1.2911	1.2819	1.2739	1.2659	1.2572	1.2496
[2O2HTMG][BF <sub>4</sub> ]	1.1663	1.1584	1.1514	1.1445	1.1365	1.1285	1.1220
[2O2HTMG][TFA]	1.1575	1.1499	1.1416	1.1336	1.1260	1.1178	1.1101
[C <sub>5</sub> HTMG][NTf <sub>2</sub> ]	1.3239	1.3153	1.3064	1.2968	1.2870	1.2778	1.2687

**Table S2** Fitting parameters for the  $T$ -dependent densities according to eqn (S1).

Ionic liquid	$a / \text{g} \cdot \text{mL}^{-1}$	$\Delta a / 10^{-3} \text{ g} \cdot \text{mL}^{-1}$	$b / 10^{-4} \text{ g} \cdot \text{mL}^{-1} \cdot \text{K}^{-1}$	$\Delta b / 10^{-6} \text{ g} \cdot \text{mL}^{-1} \cdot \text{K}^{-1}$	$R^2$
[2O2HTMG][FSI]	1.5362	3.0	8.2536	8.98	0.9994
[2O2HTMG][NTf <sub>2</sub> ]	1.6473	3.3	9.4099	9.95	0.9994
[2O2HTMG][BETI]	1.7504	3.0	10.400	9.02	0.9996
[2O2HTMG][OTf]	1.4814	4.2	8.0492	12.6	0.9988
[2O2HTMG][PF <sub>6</sub> ]	1.5469	2.3	8.3115	6.88	0.9997
[2O2HTMG][BF <sub>4</sub> ]	1.3871	2.7	7.4105	8.31	0.9994
[2O2HTMG][TFA]	1.3939	1.1	7.9283	3.37	0.9999
[C <sub>5</sub> HTMG][NTf <sub>2</sub> ]	1.6014	2.5	9.2898	7.46	0.9997

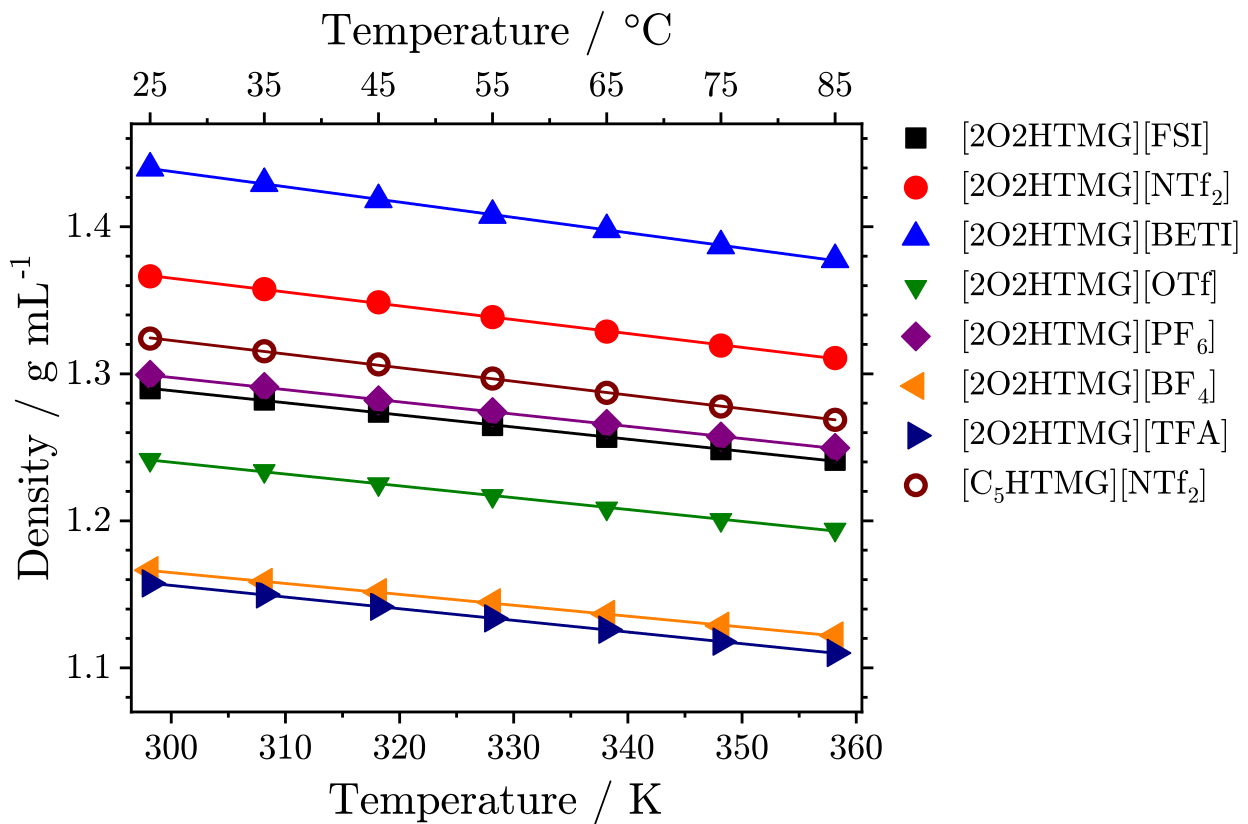


**Figure S2** Temperature-dependent densities of the guanidinium ionic liquids. Drawn lines are the linear fits following eqn (S1).

## S4 Viscosity

Experimental values for the viscosity  $\eta$  are given in Table S3. Fitting parameters for the Vogel-Fulcher-Tamman eqn (S2) are given in Table S4.

$$\eta = \eta_0 \cdot \exp\left(\frac{B_\eta}{T - T_{0,\eta}}\right) \quad (\text{S2})$$

**Table S3** Experimental viscosities  $\eta$  at the stated temperatures given in mPa · s.

$T / ^\circ\text{C}$	[2O2HTMG]						[C <sub>5</sub> HTMG]	
	[FSI]	[NTf <sub>2</sub> ]	[BETI]	[OTf]	[PF <sub>6</sub> ]	[BF <sub>4</sub> ]	[TFA]	[NTf <sub>2</sub> ]
25	50.36	58.47	116.4	172.1	505.1	264.5	137.0	91.39
30	41.08	46.49	87.73	127.3	347.4	188.1	101.3	70.95
35	33.98	37.64	67.87	96.68	246.9	137.8	76.83	56.19
40	28.54	31.00	53.55	75.05	180.7	103.6	59.81	45.34
45	24.21	25.84	42.97	59.32	135.38	79.62	47.4	37.00
50	20.78	21.85	35.07	47.83	104.0	62.52	38.29	30.66
55	18.01	18.67	29.03	39.11	81.36	50.01	31.37	25.72
60	15.73	16.10	24.33	32.40	64.77	40.65	26.07	21.78
65	13.87	14.04	20.66	27.23	52.57	33.56	22.04	18.73
70	12.32	12.33	17.70	23.11	43.23	28.04	18.83	16.18
75	11.02	10.92	15.35	19.82	36.06	23.74	16.35	14.16
80	9.91	9.73	13.37	17.17	30.42	20.31	14.20	12.47
85	8.96	8.73	11.77	14.99	25.92	17.54	12.50	11.04
90	8.16	7.88	10.45	13.20	22.31	15.33	11.07	9.85
95	7.48	7.17	9.32	11.70	19.36	13.42	9.83	8.84
100	6.85	6.56	8.35	10.42	16.94	11.89	8.80	7.96
105	6.30	5.98	7.53	9.34	14.94	10.59	7.79	7.22

**Table S4** Fitting parameters for the  $T$ -dependent viscosity  $\eta$  according to eqn (S2).

Ionic liquid	$\eta_0 / 10^{-1} \text{ mPa} \cdot \text{s}$	$\Delta\eta_0 / 10^{-3} \text{ mPa} \cdot \text{s}$	$B_\eta / \text{K}$	$\Delta B_\eta / \text{K}$	$T_{0,\eta} / \text{K}$	$\Delta T_{0,\eta} / \text{K}$	$R^2$
[2O2HTMG][FSI]	2.381	2.3	675.6	3.0	172.0	0.3	> 0.99999
[2O2HTMG][NTf <sub>2</sub> ]	2.045	1.9	670.7	2.6	179.6	0.3	> 0.99999
[2O2HTMG][BETI]	1.681	2.3	728.0	3.5	186.8	0.0	> 0.99999
[2O2HTMG][OTf]	1.730	1.1	757.1	1.7	188.5	0.1	> 0.99999
[2O2HTMG][PF <sub>6</sub> ]	1.629	3.0	821.7	4.3	185.9	0.3	> 0.99999
[2O2HTMG][BF <sub>4</sub> ]	1.659	2.9	759.1	4.1	195.2	0.3	> 0.99999
[2O2HTMG][TFA]	2.070	5.0	664.9	5.8	195.8	0.5	0.99997
[C <sub>5</sub> HTMG][NTf <sub>2</sub> ]	1.523	3.0	777.2	5.5	176.7	0.5	> 0.99999

## S5 Specific conductivity

Experimental values for the specific conductivity  $\kappa$  are given Table S5 and plotted in Figure S3, VFT-fitting parameters according to eqn (S3) for the  $T$ -dependent values are given in Table S6.

$$\kappa = \kappa_0 \cdot \exp\left(\frac{B_\kappa}{T - T_{0,\kappa}}\right) \quad (\text{S3})$$

**Table S5** Experimental specific conductivities  $\kappa$  at the stated temperatures given in  $\text{mS} \cdot \text{cm}^{-1}$ .

$T / ^\circ\text{C}$	[O2HTMG]						[C <sub>5</sub> HTMG]	
	[FSI]	[NTf <sub>2</sub> ]	[BETI]	[OTf]	[PF <sub>6</sub> ]	[BF <sub>4</sub> ]	[TFA]	[NTf <sub>2</sub> ]
25	4.085	2.391	1.031	1.039	0.553	1.112	0.821	1.660
30	4.847	2.931	1.325	1.368	0.779	1.528	1.064	2.078
35	5.734	3.568	1.662	1.754	1.077	2.043	1.355	2.555
40	6.731	4.279	2.060	2.211	1.436	2.669	1.690	3.110
45	7.818	5.061	2.505	2.738	1.868	3.415	2.075	3.732
50	8.972	5.905	3.015	3.347	2.382	4.283	2.512	4.415
55	10.22	6.844	3.583	4.032	2.993	5.242	3.010	5.154
60	11.55	7.820	4.198	4.783	3.687	6.357	3.550	5.967
65	12.95	8.882	4.885	5.575	4.481	7.609	4.153	6.851
70	14.43	10.01	5.592	6.473	5.380	8.912	4.805	7.806
75	15.98	11.23	6.415	7.510	6.370	10.41	5.512	8.821
80	17.64	12.50	7.277	8.571	7.457	12.05	6.301	9.875
85	19.35	13.82	8.182	9.708	8.636	13.80	7.149	11.02
90	21.12	15.20	9.131	10.92	9.915	15.65	8.043	12.21
95	22.95	16.59	10.13	12.22	11.30	17.54	9.006	13.45
100	24.82	18.10	11.18	13.58	12.79	19.62	10.03	14.75

**Table S6** Fitting parameters for the  $T$ -dependent specific conductivities  $\kappa$  according to eqn (S3).

Ionic liquid	$\kappa_0 / \text{mS} \cdot \text{cm}^{-1}$	$\Delta\kappa_0 / \text{mS} \cdot \text{cm}^{-1}$	$B_\kappa / \text{K}$	$\Delta B_\kappa / \text{K}$	$T_{0,\kappa} / \text{K}$	$\Delta T_{0,\eta} / \text{K}$	$R^2$
[2O2HTMG][FSI]	627.2	12.2	-673.4	6.9	164.6	0.9	> 0.99999
[2O2HTMG][NTf <sub>2</sub> ]	467.2	11.1	-643.6	7.8	178.0	1.0	0.99999
[2O2HTMG][BETI]	454.0	15.2	-707.9	10.8	182.0	1.2	0.99999
[2O2HTMG][OTf]	666.3	26.9	-743.8	12.9	184.4	1.4	0.99999
[2O2HTMG][PF <sub>6</sub> ]	825.0	14.3	-725.9	5.1	198.9	0.5	> 0.99999
[2O2HTMG][BF <sub>4</sub> ]	792.4	28.5	-633.2	10.3	201.9	1.2	0.99999
[2O2HTMG][TFA]	670.5	25.0	-847.7	12.9	171.5	1.3	0.99999
[C <sub>5</sub> HTMG][NTf <sub>2</sub> ]	492.1	6.9	-684.9	4.6	177.9	0.5	> 0.99999

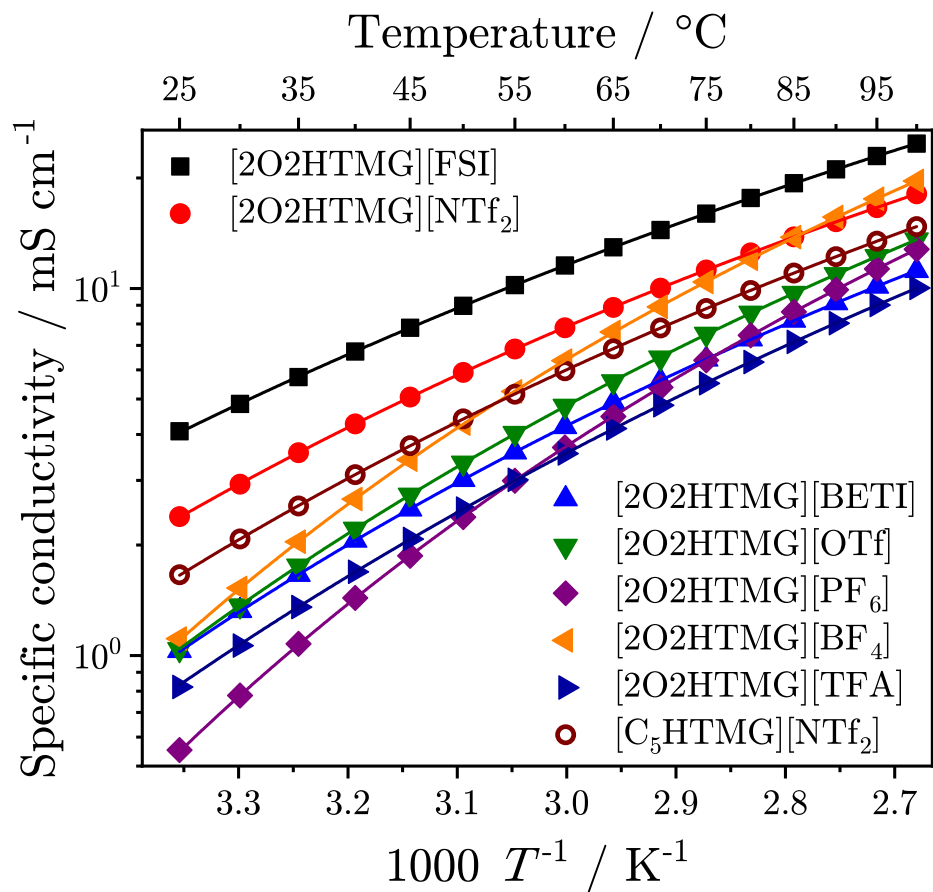


**Figure S3** Experimental specific conductivity of the guanidinium ionic liquids as a function of temperature. Drawn lines are the VFT fits according to eqn (S3).

## S6 Molar Conductivity

Values of the molar conductivity are given in Table S7, fitting parameters according to eqn (S4) can be found in Table S8.

$$\Lambda_M = \Lambda_{M,0} \cdot \exp\left(\frac{B_{\Lambda_M}}{T - T_{0,\Lambda_M}}\right) \quad (\text{S4})$$

**Table S7** Experimental molar conductivities  $\Lambda_M$  at the stated temperatures given in  $\text{S} \cdot \text{cm}^2 \cdot \text{mol}^{-1}$ .

T / °C	[2O2HTMG]						[C <sub>5</sub> HTMG]	
	[FSI]	[NTf <sub>2</sub> ]	[BETI]	[OTf]	[PF <sub>6</sub> ]	[BF <sub>4</sub> ]	[TFA]	[NTf <sub>2</sub> ]
25	1.166	0.820	0.407	0.282	0.142	0.262	0.214	0.585
30	1.389	1.008	0.525	0.373	0.200	0.362	0.278	0.734
35	1.648	1.232	0.661	0.480	0.278	0.485	0.355	0.906
40	1.941	1.482	0.822	0.607	0.372	0.636	0.444	1.107
45	2.262	1.759	1.003	0.754	0.486	0.816	0.548	1.333
50	2.604	2.059	1.212	0.924	0.621	1.027	0.665	1.583
55	2.974	2.395	1.445	1.118	0.783	1.260	0.800	1.854
60	3.373	2.746	1.700	1.330	0.968	1.534	0.947	2.154
65	3.796	3.130	1.985	1.555	1.180	1.842	1.112	2.482
70	4.244	3.542	2.281	1.812	1.421	2.164	1.291	2.839
75	4.715	3.986	2.627	2.109	1.688	2.537	1.486	3.220
80	5.221	4.453	2.991	2.415	1.983	2.945	1.704	3.617
85	5.745	4.942	3.375	2.745	2.304	3.384	1.941	4.050
90	6.293	5.454	3.781	3.098	2.654	3.850	2.191	4.506
95	6.860	5.974	4.212	3.479	3.035	4.331	2.462	4.981
100	7.446	6.542	4.666	3.878	3.447	4.860	2.752	5.481

**Table S8** Fitting parameters for the  $T$ -dependent molar conductivities  $\Lambda_M$  according to eqn (S4).

Ionic liquid	$\Lambda_{M,0}$ / $S \cdot cm^2 \cdot mol^{-1}$	$\Delta\Lambda_{M,0}$ / $S \cdot cm^2 \cdot mol^{-1}$	$B_{\Lambda_{M,0}}$ / K	$\Delta B_{\Lambda_{M,0}}$ / K	$T_{0,\Lambda_{M,0}}$ / K	$\Delta T_{0,\Lambda_{M,0}}$ / K	$R^2$
[2O2HTMG][FSI]	233.6	4.6	-736.8	7.2	159.3	0.9	> 0.99999
[2O2HTMG][NTf <sub>2</sub> ]	209.3	5.3	-693.1	8.6	173.2	1.1	0.99999
[2O2HTMG][BETI]	236.2	8.2	-766.8	11.7	177.7	1.3	0.99999
[2O2HTMG][OTf]	231.7	21.6	-786.6	14.1	180.8	1.5	0.99999
[2O2HTMG][PF <sub>6</sub> ]	265.1	4.5	-768.4	5.2	196.2	0.5	> 0.99999
[2O2HTMG][BF <sub>4</sub> ]	232.0	8.9	-672.7	11.5	199.1	1.3	0.99999
[2O2HTMG][TFA]	232.2	10.4	-914.1	16.2	167.1	1.6	0.99999
[C <sub>5</sub> HTMG][NTf <sub>2</sub> ]	228.2	6.0	-745.2	7.0	173.3	0.5	> 0.99999

## S7 Walden Relation

Linear fitting of the logarithm of  $\eta^{-1}$  in Poise vs. the logarithm of the molar conductivity  $\Lambda_M$  in  $\text{S} \cdot \text{cm}^2 \cdot \text{mol}^{-1}$  according to eqn (S5).<sup>4,5</sup> The results are given in Table S9

$$\log\left(\frac{\Lambda_M}{\text{S} \cdot \text{cm}^2 \cdot \text{mol}^{-1}}\right) = \log(C) + t \cdot \log\left(\frac{0.1 \text{ Pa} \cdot \text{s}}{\eta}\right) \quad (\text{S5})$$

**Table S9** Fitting parameters for Walden plot according to eqn (S5).

Ionic liquid	$\log C / 10^{-1}$	$\Delta \log C / 10^{-3}$	$t$	$\Delta t / 10^{-3}$	$R^2$
[2O2HTMG][FSI]	-2.190	2.5	0.9334	3.0	0.9999
[2O2HTMG][NTf <sub>2</sub> ]	-3.124	1.5	0.9500	1.8	> 0.9999
[2O2HTMG][BETI]	-3.359	1.7	0.9284	2.4	0.9999
[2O2HTMG][OTf]	-3.324	1.0	0.9347	1.6	> 0.9999
[2O2HTMG][PF <sub>6</sub> ]	-1.891	0.4	0.9399	0.8	> 0.9999
[2O2HTMG][BF <sub>4</sub> ]	-1.826	0.4	0.9411	0.8	> 0.9999
[2O2HTMG][TFA]	-5.578	4.0	0.9326	6.0	0.9994
[C <sub>5</sub> HTMG][NTf <sub>2</sub> ]	-2.717	0.8	0.9182	1.1	> 0.9999

The ionicity as deviation from the bisection in the Walden plot, the Walden ionicity  $\Delta W$  as calculated by eqn (S6) in dependence of  $T$  is summarized in Table S10 and plotted in Fig S4.

$$\Delta W = \frac{\Lambda_M^{\exp}(T)}{S \cdot \text{cm}^2 \cdot \text{mol}^{-1}} \cdot \frac{\eta^{\exp}(T)}{0.1 \text{ Pa} \cdot \text{s}} \quad (\text{S6})$$

**Table S10** Ionicities  $\Delta W$  as obtained from the Walden plot following eqn S6. Values are given in percent.

$T / ^\circ\text{C}$	[2O2HTMG]							$[\text{C}_5\text{HTMG}]$ [NTf <sub>2</sub> ]
	[FSI]	[NTf <sub>2</sub> ]	[BETI]	[OTf]	[PF <sub>6</sub> ]	[BF <sub>4</sub> ]	[TFA]	
25	58.7	47.9	47.4	48.6	71.6	69.4	29.3	53.4
30	57.0	46.9	46.0	47.5	69.6	68.0	28.1	52.1
35	56.0	46.4	44.8	46.4	68.6	66.8	27.3	50.9
40	55.4	45.9	44.0	45.5	67.2	65.9	26.6	50.2
45	54.7	45.4	43.1	44.7	65.7	65.0	26.0	49.3
50	54.1	45.0	42.5	44.2	64.5	64.2	25.5	48.5
55	53.6	44.7	42.0	43.7	63.7	63.0	25.1	47.7
60	53.0	44.2	41.4	43.1	62.7	62.3	24.7	46.9
65	52.6	44.0	41.0	42.3	62.0	61.8	24.5	46.5
70	52.3	43.7	40.4	41.9	61.4	60.7	24.3	45.9
75	52.0	43.5	40.3	41.8	60.9	60.2	24.3	45.6
80	51.7	43.3	40.0	41.5	60.3	59.8	24.2	45.1
85	51.5	43.2	39.7	41.2	59.7	59.4	24.3	44.7
90	51.3	43.0	39.5	40.9	59.2	59.0	24.2	44.4
95	51.3	42.8	39.3	40.7	58.8	58.1	24.2	44.0
100	51.0	42.9	39.0	40.4	58.4	57.8	24.2	43.6

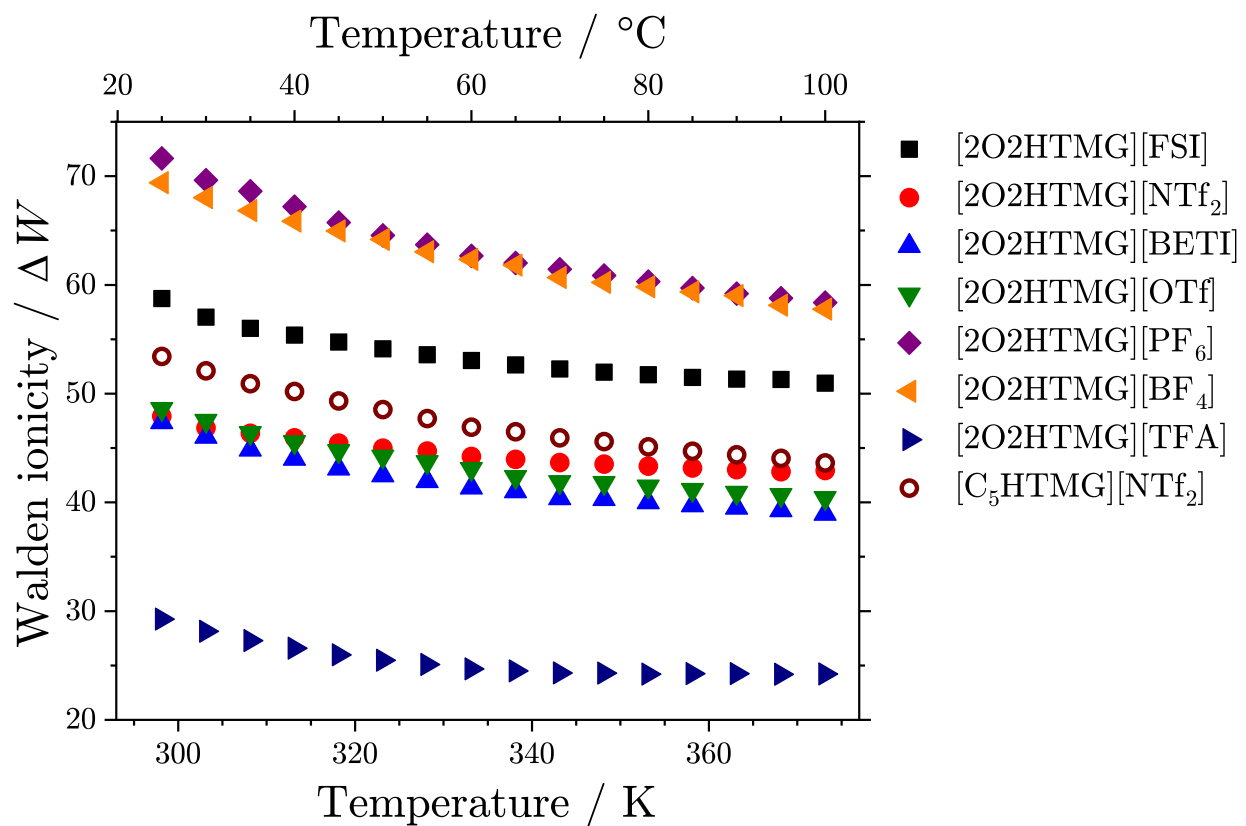


**Figure S4** Ionicity  $\Delta W$  as obtained by the Walden relation eqn (S6) in dependence of temperature.

## S8 Small Angle X-ray Scattering

Radially averaged small angle X-ray scattering (SAXS) profiles of the investigated guanidinium ionic liquids are shown in Figure S5. The peak positions and corresponding real space distances are given in the main manuscript.

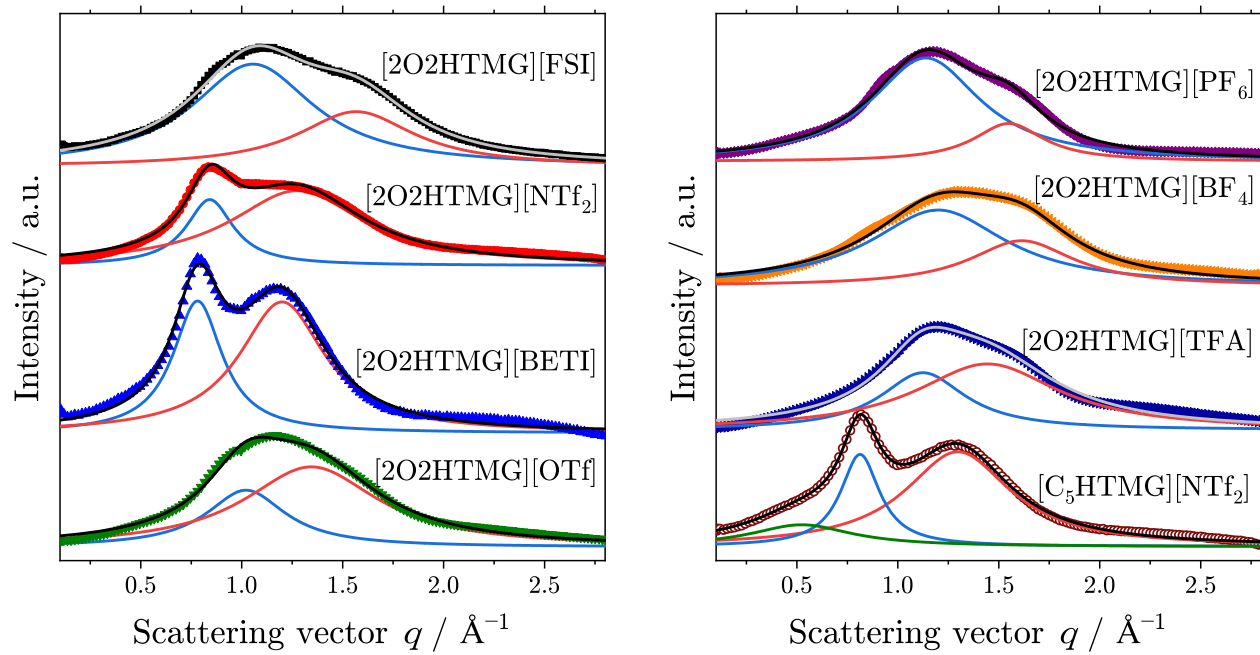


**Figure S5** Radially averaged small angle X-ray scattering patterns recorded at ambient temperature. Lorentzian functions for the fitting of the peaks are included. Green curves are for the ‘polarity peak’ and only found for the sample  $[C_5\text{HTMG}][\text{NTf}_2]$ , although less pronounced. Blue curves are for the ‘charge peak’ and red Lorentz function for the ‘adjacency peak’.<sup>6</sup>

The peak positions of the charge peak (interactions and geometric effects) showed a linear correlation to the ion distances, calculated as the sum of the ion radii,  $r_{\text{cation}} + r_{\text{anion}}$  (interaction free, unperturbed system) obtained from *ab initio* calculations,<sup>7–9</sup> Figure S6. Differences are decreasing with increasing anion size, indicating that geometric factors are causing the lower values of the cation-anion distance in liquid state.

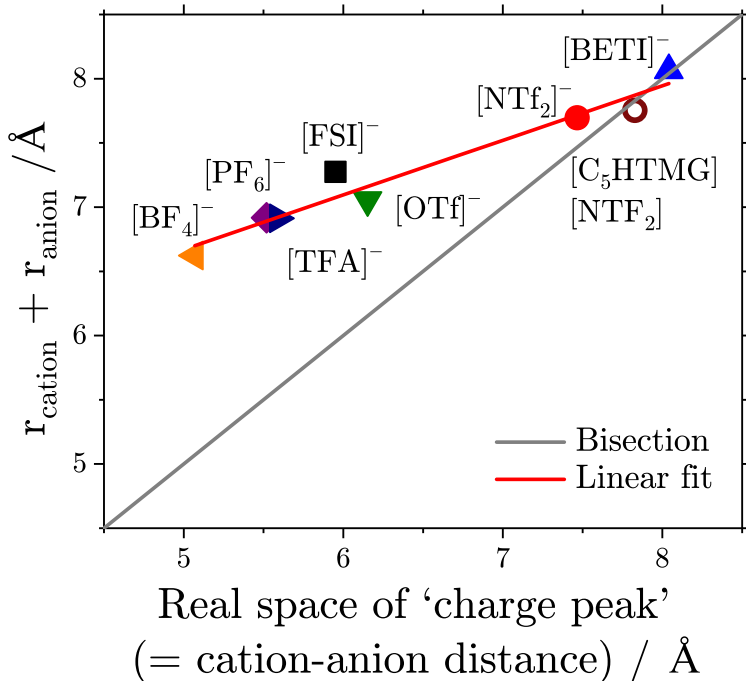


**Figure S6** Correlation between cation-anion distance in the  $[\text{O}2\text{HTMG}]^+$  ionic liquids at ambient temperature (real space distance of the 'charge peak') and the sum of the ion radii obtained from *ab initio* calculations. Coefficient of determination  $R^2 = 0.95$ .

## S9 Proton Affinity

Proton affinities were calculated by subtracting the energy of the protonated species (the acid) from the energy of the corresponding anion, Table S11.

**Table S11** Proton affinity for the acids by *ab initio* calculations as internal energy and Gibbs energy at the B3LYP/6-311+G(d,p) level of theory.

Acid	Internal / kJ mol <sup>-1</sup>	Gibbs energy / kJ mol <sup>-1</sup>
HFSI	1243.143	1211.676
HNTf <sub>2</sub>	1259.514	1228.310
HBETI	1251.038	1221.923
HOTf	1279.861	1250.470
HPF <sub>6</sub>	1180.021	1167.260
HBF <sub>4</sub>	1238.143	1225.318
HTFA	1369.554	1332.971

## S10 Additional Computations

### S10.1 Ion Volumes and Radii

Volumes were obtained by integrating the 0.001 isosurface of the electron density with a 0.15 bohr spacing of grid points using the Multiwfn software package.<sup>7,8</sup> The radii  $r$  were estimated from the Volumes  $V$  assuming a sphere,  $r_i = \left(\frac{3V}{4\pi}\right)^{1/3}$ . Values for the ion radii  $r_i$  are given in Table S12.

**Table S12** Radii  $r_i$  of the ions as obtained by *ab initio* calculations.

Ion	Radius $r_i$ / Å
[2O2HTMG] <sup>+</sup>	4.033
[C <sub>5</sub> HTMG] <sup>+</sup>	4.092
[FSI] <sup>-</sup>	3.241
[NTf <sub>2</sub> ] <sup>-</sup>	3.686
[BETI] <sup>-</sup>	4.031
[OTf] <sup>-</sup>	3.022
[PF <sub>6</sub> ] <sup>-</sup>	2.883
[BF <sub>4</sub> ] <sup>-</sup>	2.589
[TFA] <sup>-</sup>	2.880

### S10.2 H-bonding criteria

For X···H contacts to be classified as H-bonding interactions, the X···H distance needs to be smaller than the sum of van der Waals radii of H and X, Table S13 , and a bond critical point (BCP) must be present. The strength of H-bonding interactions is quantified via electronic properties from quantum theory of atoms in molecules (QTAIM) and natural bond orbital (NBO) calculations, Table S14.<sup>10</sup>  $\rho$  is the electron density,  $\nabla^2\rho$  is the Laplacian of the electron density (the second derivative of the electron density with respect to the  $x$ ,  $y$  and  $z$  coordinates in Cartesian space),  $H$  is the total energy density,  $E^{(2)}$  is the stabilization energy due to orbital donor-acceptor interactions as defined by the second order perturbation theory of NBO analysis and  $E_{\text{HB}}$  is the hydrogen bond energy.  $E^{(2)}$  has been determined for interactions between lone electron pair orbitals donating electron density into antibonding C-H/N-H orbitals.  $E_{\text{HB}}$  can be estimated from different electronic structure properties, equations S7 to S10.<sup>11,12</sup>  $V$  in eqn S7 is the potential energy density.

**Table S13** Van der Waals radii of H, N, O and F atoms in Å.

H	N	O	F
1.10	1.55	1.52	1.47
N+H	O+H	F+H	
2.65	2.62	2.57	

**Table S14** Electronic structure property criteria for the quantitative characterizations of H-bonds.

	strong	moderate	weak
1.10	1.55	1.52	1.47
$\rho_{\text{BCP}} / \text{a.u.}$	> 0.05	0.02 - 0.05	0.02 - 0.002
$\nabla^2 \rho_{\text{BCP}} / \text{a.u.}$	+ve	+ve or -ve	+ve and small (<0.01)
$H_{\text{BCP}}$	< 0	< 0	>0
$E^{(2)} / \text{kJ mol}^{-1}$	> 150	30-150	< 30
$E_{\text{HB}} / \text{kJ mol}^{-1}$	63 - 167	17 - 63	< 17

$$E^1 / \text{kJ mol}^{-1} = \frac{V_{\text{BCP}}}{2} \quad (\text{S7})$$

$$E^2 / \text{kJ mol}^{-1} = (-357.73 \cdot \rho_{\text{BCP}} + 2.6182) \cdot 4.184 \quad (\text{S8})$$

$$E^3 / \text{kJ mol}^{-1} = (-223.08 \cdot \rho_{\text{BCP}} + 0.7423) \cdot 4.184 \quad (\text{S9})$$

$$E^4 / \text{kJ mol}^{-1} = (-332.34 \cdot \rho_{\text{BCP}} - 1.0661) \cdot 4.184 \quad (\text{S10})$$

## S10.3 Isolated Cations

### S10.3.1 Potential Energy Surfaces

Potential energy surface (PES) for the alkylated cation  $[\text{C}_4\text{HTMG}]^+$  with conformation of the minimum energy structures are shown in Figure S7. The PES and conformations of the minimum energy structures of the ether cation  $[\text{2O1HTMG}]^+$  are given in the main manuscript. For each of the PES, a z-matrix was created with the two dihedrals of interest as variables. These two dihedrals were then set to all combinations from  $0^\circ$  to  $360^\circ$ , in steps of  $10^\circ$ . The resulting structures were optimized under partial restraints (with the two dihedral angles being frozen) at the B3LYP-GD3BJ/6-311+G(d,p) level of theory, followed by a single point calculation at the frozen core MP2/cc-pVTZ level of theory.

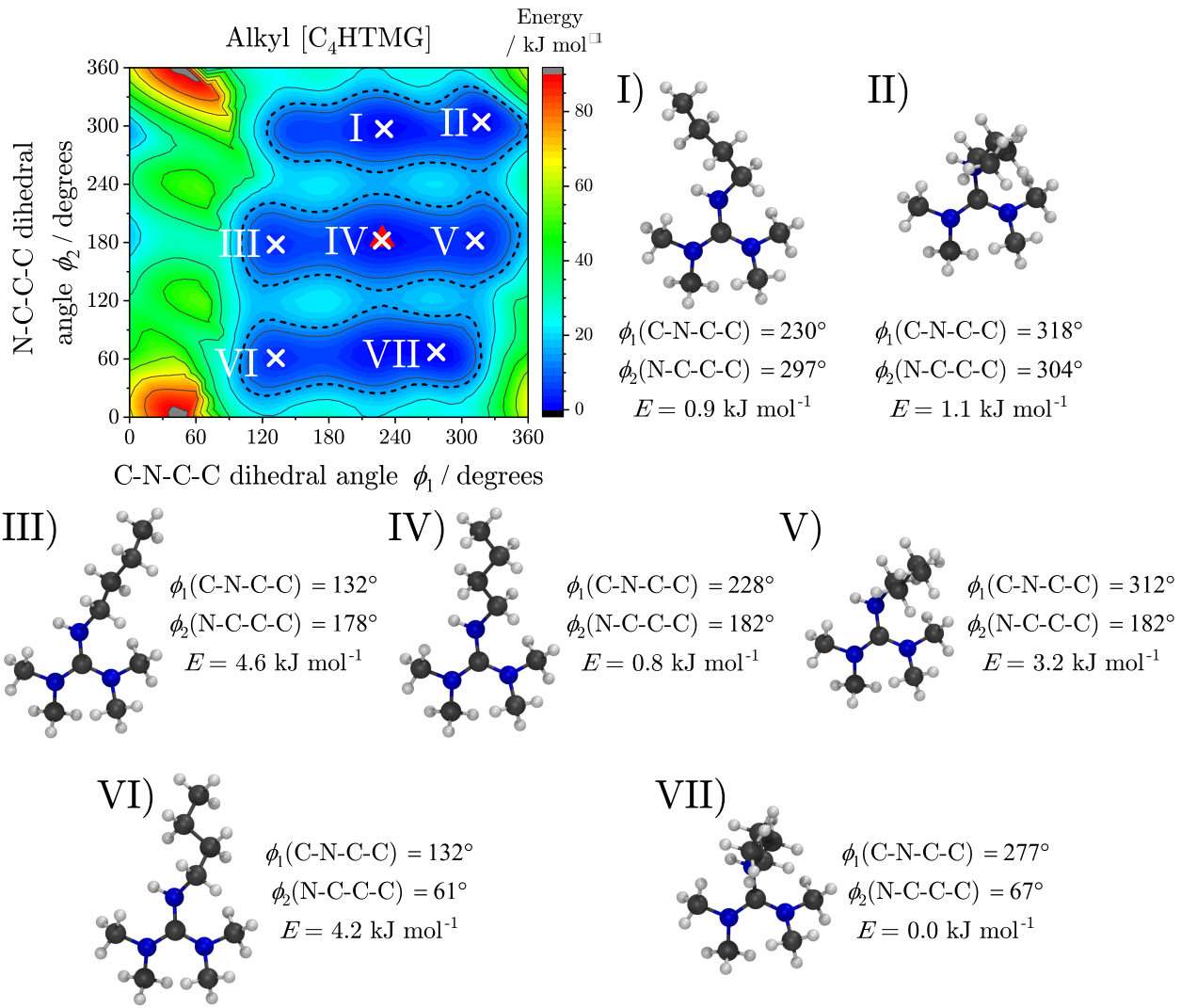


**Figure S7** Potential energy surfaces for the C–N–C–C dihedral angle  $\phi_1$  vs. the N–C–C–C dihedral angle  $\phi_2$  of the [C<sub>4</sub>HTMG]<sup>+</sup> cation. The white crosses show minimum energy structures, the red triangles mark the dihedral angles obtained from the single crystal structure analysis. Dashed lines are the 15 kJ mol<sup>-1</sup> limit for the thermally accessible regions of the potential energy surface. Conformation of the seven minimum energy structures for the alkylated cation [C<sub>4</sub>HTMG]<sup>+</sup>. Energies given are at the MP2/cc-pVTZ//B3LYP-GD3BJ/6-311+G(d,p) level of theory.

### S10.3.2 $[2\text{O}1\text{HTMG}]^+$

Three different conformers were studied, two energetically degenerate low energy conformers ( $[2\text{O}1\text{HTMG}]^+$  286\_56 and 229\_311) and a slightly higher energy conformer ( $[2\text{O}1\text{HTMG}]^+$ , 8 kJ mol<sup>-1</sup>), Figure S8. Thereby the values indicate the dihedral angles  $\phi_1$  (C-N-C-C) and  $\phi_2$  (N-C-C-O) as indicated in Figure 1 of the main manuscript. Based on the shortest O···H contact in  $[2\text{O}1\text{HTMG}]^+$  286\_56 (2.72 Å), no H-bonding interaction is present. The other two conformers ( $[2\text{O}1\text{HTMG}]^+$  229\_311 and  $[2\text{O}1\text{HTMG}]^+$  135\_297) show shorter O···H contacts and electronic structure properties, Table S15, which classify those O···H contacts as weak H-bonds. An effect different from H-bonding must be stabilizing the 286\_56 conformer.

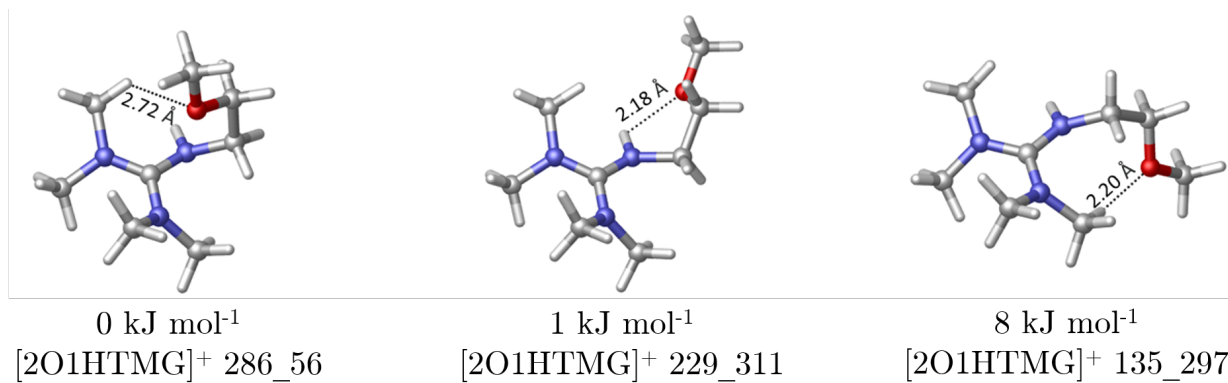


**Figure S8** B3LYP-GD3BJ/6-311+G(d,p) optimized geometries of  $[2\text{O}1\text{HTMG}]^+$ .

**Table S15** Electronic structure properties at the B3LYP-GD3BJ/6-311+G(d,p) level of theory for the characterization of intramolecular H-bond strength in different  $[2\text{O}1\text{HTMG}]^+$  conformers.

	$[2\text{O}1\text{HTMG}]^+$ conformers		
	286_56	229_311	135_297
$\rho_{\text{BCP}} / \text{a.u.}$	0.0067	0.0180	0.0159
$\nabla^2\rho_{\text{BCP}} / \text{a.u}$	0.0218	0.0843	0.0566
$H_{\text{BCP}} / \text{a.u}$	0.0006	0.0035	0.0020
$V_{\text{BCP}} / \text{a.u}$	-0.0042	-0.0141	-0.0102
$E^{(2)} / \text{kJ mol}^{-1}$	—	6.69	10.75
$E_{\text{HB}}^1 / \text{kJ mol}^{-1}$	-5.5	-18.5	-13.4
$E_{\text{HB}}^2 / \text{kJ mol}^{-1}$	0.9	-16.0	-12.8
$E_{\text{HB}}^3 / \text{kJ mol}^{-1}$	-3.1	-13.7	-11.7
$E_{\text{HB}}^4 / \text{kJ mol}^{-1}$	-13.8	-29.5	-26.6

The interactions between the methoxy group and the cation ‘core’ were examined via intramolecular SAPT(0) calculations, Figure S9. The methylene group was chosen

as the linker (fragment C) between the methoxy group (fragment A) and the remaining cation core (fragment B). The stabilization of the  $[2\text{O}1\text{HTMG}]^+$  286\_56 conformer by the methoxy-'core' interactions is roughly double as negative ( $-23 \text{ kJ mol}^{-1}$ ) as for the two other conformers ( $-13$  and  $-10 \text{ kJ mol}^{-1}$ ). In comparison to the  $[2\text{O}1\text{HTMG}]^+$  286\_56 conformer, the  $[2\text{O}1\text{HTMG}]^+$  229\_311 and  $[2\text{O}1\text{HTMG}]^+$  135\_297 conformers are less stabilized by dispersion ( $-14 \text{ kJ mol}^{-1}$  vs.  $-8 \text{ kJ mol}^{-1}$  and  $-10 \text{ kJ mol}^{-1}$ ) and show greater destabilization through exchange interactions ( $16 \text{ kJ mol}^{-1}$  vs.  $22 \text{ kJ mol}^{-1}$ ). A slight variation in attractive electrostatics also contributes to the stabilization of the  $[2\text{O}1\text{HTMG}]^+$  286\_56 conformer ( $-13 \text{ kJ mol}^{-1}$  vs.  $-10 \text{ kJ mol}^{-1}$  and  $-12 \text{ kJ mol}^{-1}$ ) while induction effects remain the same across all three conformers ( $-11 \text{ kJ mol}^{-1}$ ). However, if intramolecular interactions between the methoxy and cation core alone were responsible for the energy differences, conformer  $[2\text{O}1\text{HTMG}]^+$  229\_311 would be expected to be roughly  $13 \text{ kJ mol}^{-1}$  higher in energy than the lowest energy geometry. Thus, secondary orbital interactions potentially play a role in precisely defining the relative ordering of the conformers, while the SAPT(0) calculated energy contributions allow to understand qualitative trends in relative energies.

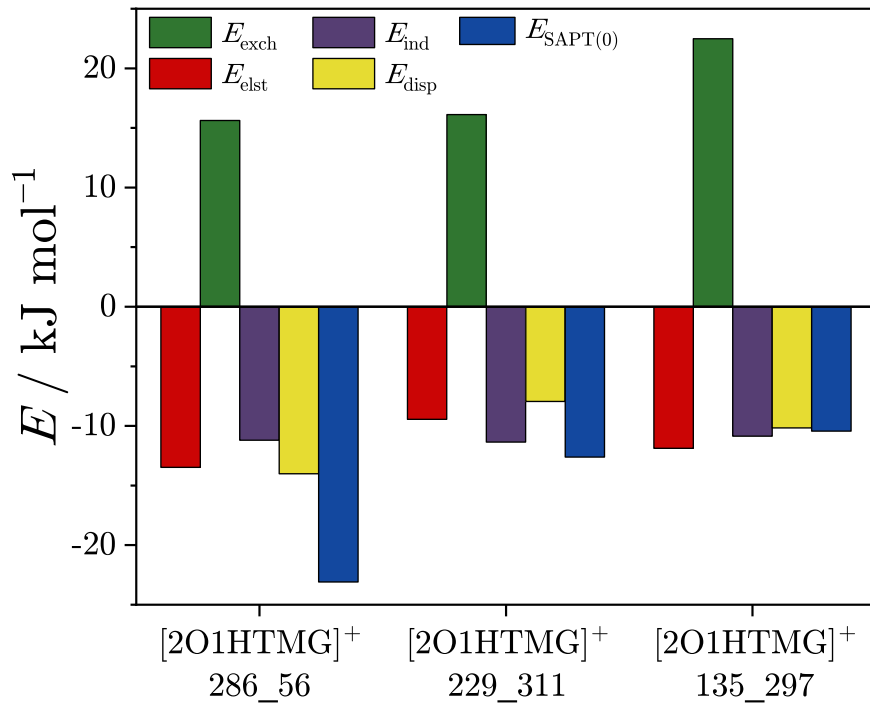


**Figure S9** Intramolecular SAPT(2) decomposition analysis with the cc-pVTZ basis set for the three stable cation conformations of the  $[2\text{O}1\text{HTMG}]^+$  cation.

### S10.3.3 Electrostatic Potential Histograms

Histograms of the electrostatic potential on the 0.001 isosurface of the electron density for the different minimum energy conformers for ether and alkyl substituted cations are shown in Figure S10. The spacing of grid points was 0.15 bohr, the electrostatic potential was sampled in 150 intervals from 167 to 544 kJ mol<sup>-1</sup> using the Multiwfn software package.<sup>7,8</sup>

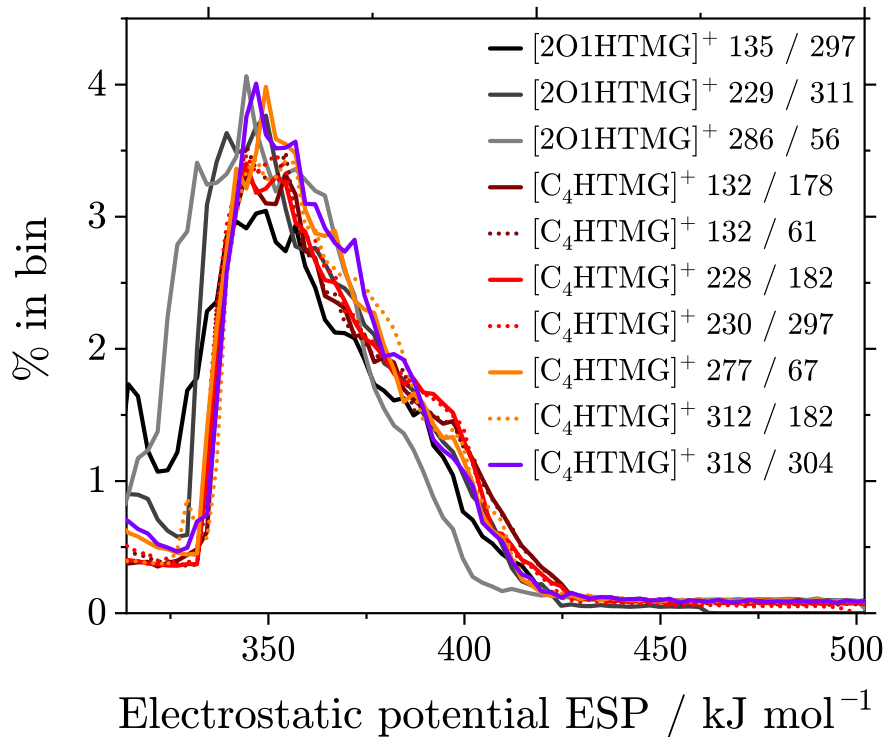


**Figure S10** Electrostatic potential histogramms for the minimum energy conformers with different dihedral angles,  $\phi_1(\text{C}-\text{N}-\text{C}-\text{C})$  and  $\phi_2(\text{N}-\text{C}-\text{C}-\text{X}; \text{with X} = \text{C}$  (alkyl side chain) or  $\text{O}$  (ether side chain)) .

## S10.4 Ion Pairs

### S10.4.1 [2O1HTMG][TFA]

A set of 30 ion pairs were randomly constructed from the isolated ion geometries (10 different IP conformations for each cation conformer). The set contains structures in the  $0 - 45 \text{ kJ mol}^{-1}$  energy range. The lowest energy ion pair contains the cation in the  $[2\text{O1HTMG}]^+ 135\_297$  conformation ([2O1HTMG][TFA] 229\_311\_c4), while a different low energy structure ( $2 \text{ kJ mol}^{-1}$ ) contains the cation in its minimum energy structure ([2O1HTMG][TFA] 286\_56\_c0), Figure S11.

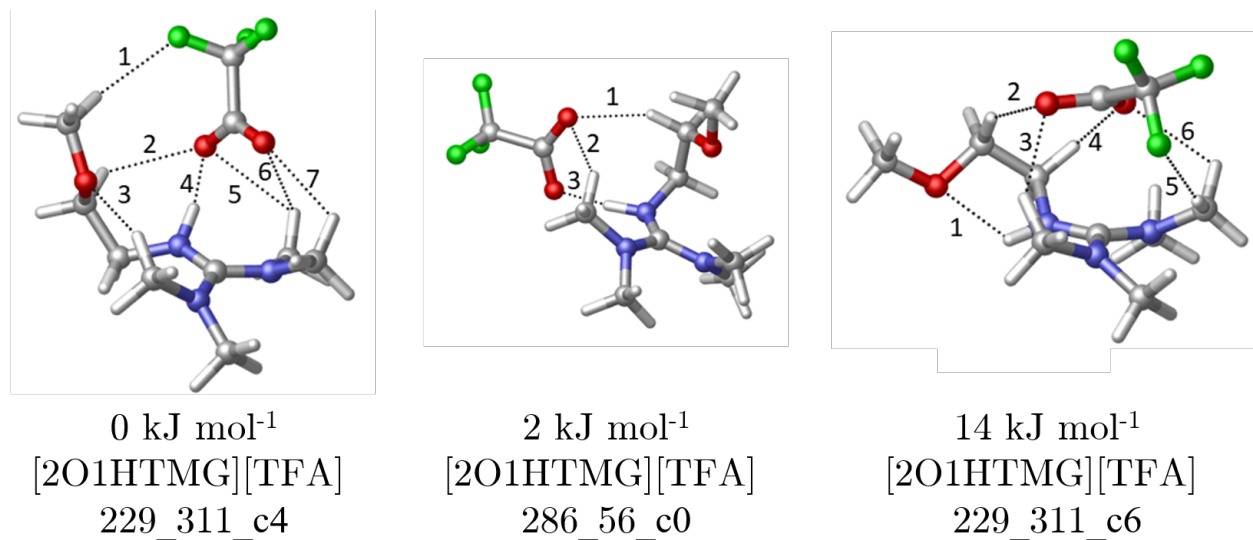


**Figure S11** [2O1HTMG][TFA] ion pairs optimized at the B3LYP-GD3BJ/6-311+G(d,p) level of theory.

The low energy difference indicates that the presence of an anion renders intramolecular interactions in the cation less important. The interaction between the N-H fragment and the anion O atom is a strong H-bond, Table 4. All other O···H and F···H contacts are weak H-bonds only.

Anion-cation interactions become less strong when the anion is oriented in a way such that it cannot interact with the N-H group. In this case a plethora of weaker H-bonding interaction with peripheral cation H atoms stabilizes the anion on top of the cation core ([2O1HTMG][TFA] 229\_311\_c6), Table S16. Such conformers are higher in energy ( $14 \text{ kJ mol}^{-1}$ ) and are less likely to be populated at room temperature.

### S10.4.2 [2O1HTMG][NTf<sub>2</sub>]

A set of 30 ion pairs were randomly constructed from the isolated ion geometries (10 different ion pairs conformations for each cation conformer, each 5 conformers with *cis* and *trans* [NTf<sub>2</sub>]<sup>-</sup>). The set contains structures in the  $0 - 51 \text{ kJ mol}^{-1}$  energy range. In agreement with the [2O1HTMG][TFA] ion pairs, the lowest energy ion pair contains the cation in the  $[2\text{O1HTMG}]^+ 135\_297$  conformation ([2O1HTMG][NTf<sub>2</sub>] 135\_297\_cis\_c2).

**Table S16** Electronic structure properties at the B3LYP-GD3BJ/6-311+G(d,p) level of theory for the characterization of intramolecular H-bond strength in different [2O1HTMG][TFA] conformers.

	$\rho_{\text{BCP}}$ / a.u.	$\nabla^2 \rho_{\text{BCP}}$ / a.u.	$H_{\text{BCP}}$ / a.u.	$V_{\text{BCP}}$ / a.u.	$E^{(2)}$ / kJ mol <sup>-1</sup>	$E_{\text{HB}}^1$ / kJ mol <sup>-1</sup>	$E_{\text{HB}}^2$ / kJ mol <sup>-1</sup>	$E_{\text{HB}}^3$ / kJ mol <sup>-1</sup>	$E_{\text{HB}}^4$ / kJ mol <sup>-1</sup>
[2O1HTMG][TFA] 229_311_c4									
BCP1	0.0068	0.0247	0.0009	-0.0045	3.06	-5.9	0.7	-3.3	-13.9
BCP2	0.0089	0.0294	0.0009	-0.0055	2.85	-7.2	-2.3	-5.2	-16.8
BCP3	0.0168	0.0597	0.0021	-0.0108	12.85	-14.2	-14.1	-12.5	-27.8
BCP4	0.0602	0.1418	-0.0122	-0.0598	184.60	-78.5	-79.2	-53.1	-88.2
BCP5	0.0076	0.0257	0.0008	-0.0048	0.29	-6.2	-0.4	-4.0	-15.0
BCP6	0.0087	0.0289	0.0008	-0.0056	0.38	-7.3	-2.1	-5.0	-16.6
[2O1HTMG][TFA] 286_56_c0									
BCP1	0.0144	0.0461	0.0014	-0.0086	11.81	-11.3	-10.6	-10.4	-24.5
BCP2	0.0136	0.0431	0.0013	-0.0081	7.08	-10.6	-9.4	-9.6	-23.3
BCP3	0.0618	0.1413	-0.0133	-0.0619	155.71	-81.2	-81.5	-54.5	-90.4
[2O1HTMG][TFA] 229_311_c6									
BCP1	0.0183	0.0820	0.0032	-0.0141	8.33	-18.5	-16.5	-14.0	-30.0
BCP2	0.0166	0.0517	0.0015	-0.0100	16.58	-13.1	-13.9	-12.4	-27.5
BCP3	0.0167	0.0582	0.0020	-0.0105	5.48	-13.8	-14.1	-12.5	-27.7
BCP4	0.0167	0.0550	0.0017	-0.0103	12.81	-13.5	-14.1	-12.5	-27.7
BCP5	0.0087	0.0312	0.0010	-0.0058	1.42	-7.6	-2.1	-5.0	-16.6
BCP6	0.0103	0.0382	0.0013	-0.0069	0.67	-9.0	-4.5	-6.5	-18.8

The anion interacts with the N-H fragment via an oxygen atom. The other oxygen, fluorine and nitrogen atoms are involved in a plethora of non-covalent interactions with the cation from a top position. The interactions include a variety of less common non H-bonding interactions (e.g. N···N, N···O, C···H, and F···O interactions, Figure S13). Two ion pairs with the curled cation conformation are also found ([2O1HTMG][NTf<sub>2</sub>] 286\_56\_trans\_c2 and [2O1HTMG][NTf<sub>2</sub>] 286\_56\_cis\_c4) but are higher in energy 14 kJ mol<sup>-1</sup> and 25 kJ mol<sup>-1</sup>. All other input geometries for ion pairs with the [2O1HTMG]<sup>+</sup> 286\_56 cation conformation optimize to ether side chain conformations which do not occupy the space on top of the cation core. The anion preferably interacts with the cation via a single H-bond with the N-H group while sitting on top of the cation core and forming multiple weak interactions with the cation core. The N-H hydrogen bonds are stronger in the two higher energy conformers but all observed H-bonding interactions with the N-H fragment are classified as medium strength H-bonds only. All other interactions are weak in nature, Table S17. A 0.001 a.u.  $\rho_{\text{BCP}}$  cut-off has been applied for visualization to reduce complexity of the QTAIM molecular graphs. However, it should be noted that multiple weak interactions

can significantly contribute to the stabilization of the ion pair if weak interactions add up constructively.

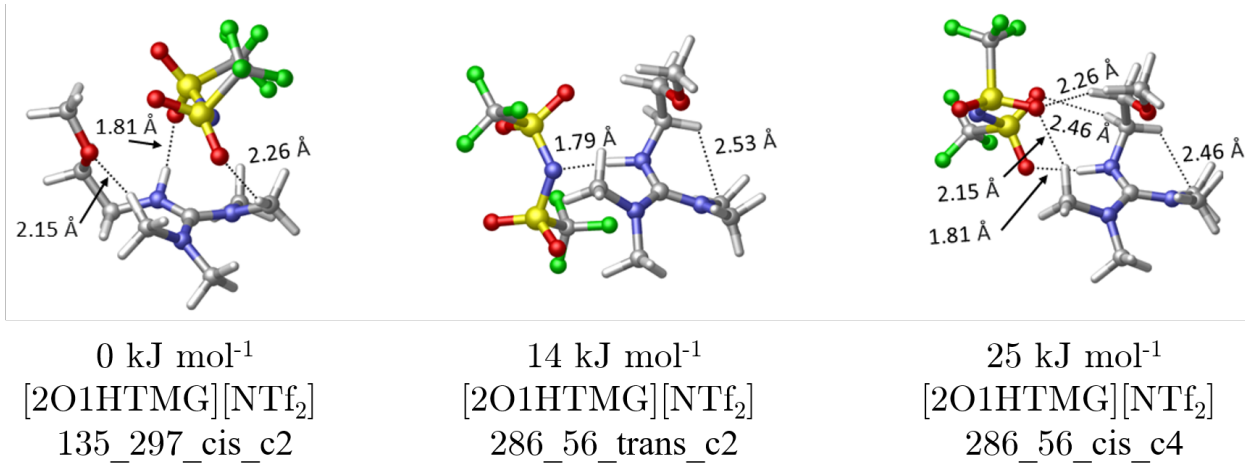


**Figure S12** [2O1HTMG][NTf<sub>2</sub>] ion pairs optimized at the B3LYP-GD3BJ/6-311+G(d,p) level of theory.

The difference in H-bonding strength between the [TFA]<sup>-</sup> and [NTf<sub>2</sub>]<sup>-</sup> based ion pairs can clearly be observed in  $\rho_{BCP}$  values of the primary H-bonding interaction of the cation NH group with the anion (0.0602 and 0.0347 a.u. for the lowest energy conformers of the [TFA]<sup>-</sup> and [NTf<sub>2</sub>]<sup>-</sup> ion pairs, respectively). This observation is reinforced by NCI plots, Figure S14. In both ion pairs there is an intramolecular area of weak H-bond interactions and extended NCI surfaces above the cation core (green in color, most likely dispersive interactions). The [NTf<sub>2</sub>]<sup>-</sup> ion pair has an additional blue colored intermolecular NCI surface for the medium strength cation-anion H-bond. The [TFA]<sup>-</sup> ion pair shows no continuous NCI surface for the intermolecular H-bonding but a ‘ring’ instead (blue colored, strongly attractive). The ring is most likely the result of the strong H-bond. The H-bond has an increased degree of covalency which significantly increases local s values. The center of the area involved in H-bonding is not longer recognized as an area of non-covalent interactions but the outer area is. Thus, only the ‘ring’ remains and the NCI framework indicates a significantly stronger H-bonding interaction (which is more covalent in nature) in the [TFA]<sup>-</sup> ion pair than in the [NTf<sub>2</sub>]<sup>-</sup> analogue.

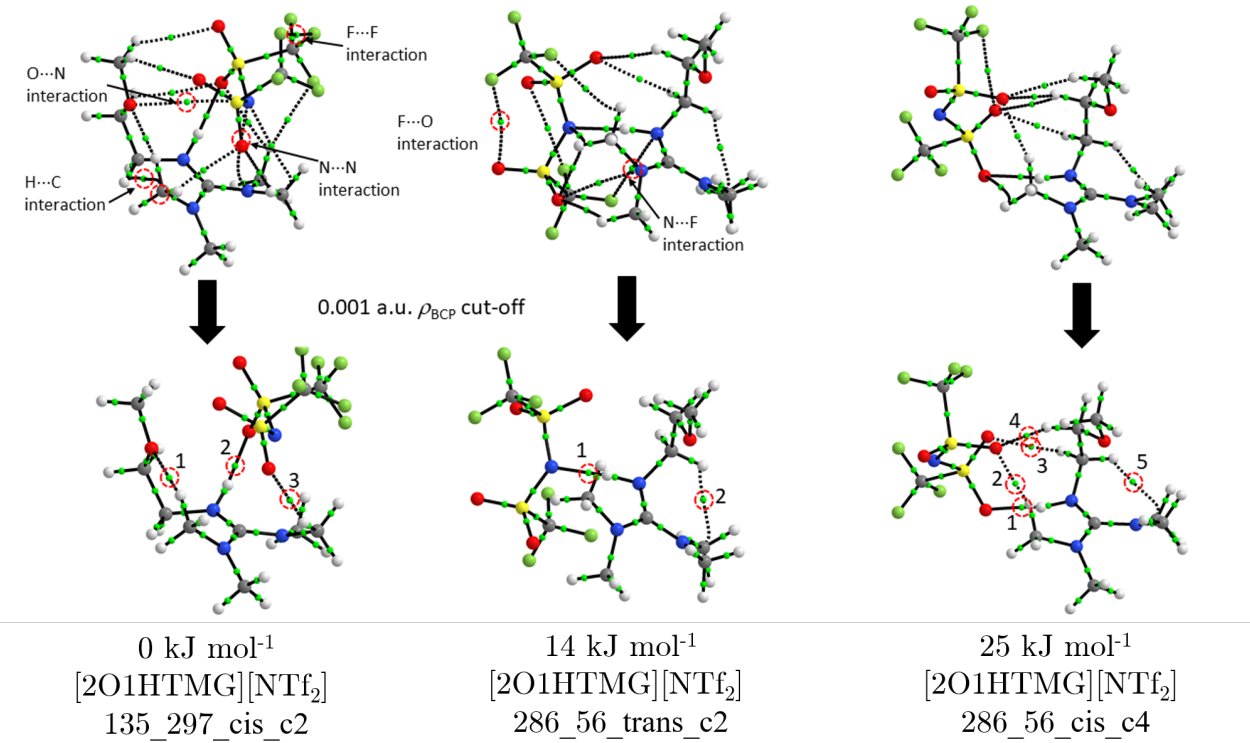


**Figure S13** QTAIM molecular graphs of selected [2O1HTMG][NTf<sub>2</sub>] ion pairs optimized at the B3LYP-GD3BJ/6-311+G(d,p) level of theory.

**Table S17** Electronic structure properties at the B3LYP-GD3BJ/6-311+G(d,p) level of theory for the characterization of intramolecular H-bond strength in different [2O1HTMG][NTf<sub>2</sub>] conformers.

	$\rho_{\text{BCP}}$ / a.u.	$\nabla^2 \rho_{\text{BCP}}$ / a.u.	$H_{\text{BCP}}$ / a.u.	$V_{\text{BCP}}$ / a.u.	$E^{(2)}$ kJ mol <sup>-1</sup>	$E_{\text{HB}}^1$ kJ mol <sup>-1</sup>	$E_{\text{HB}}^2$ kJ mol <sup>-1</sup>	$E_{\text{HB}}^3$ kJ mol <sup>-1</sup>	$E_{\text{HB}}^4$ kJ mol <sup>-1</sup>
[2O1HTMG][NTf <sub>2</sub> ] 135_297_cis_c2									
BCP1	0.0174	0.0633	0.0022	-0.0114	14.24	-15.0	-15.1	-13.1	-28.7
BCP2	0.0347	0.1237	0.0005	-0.03	75.91	-39.4	-41.0	-29.3	-52.7
BCP3	0.0144	0.0499	0.0017	-0.0091	10.47	-11.9	-10.6	-10.3	-24.5
[2O1HTMG][NTf <sub>2</sub> ] 286_56_trans_c2									
BCP1	0.0426	0.1105	-0.0049	-0.0373	111.95	-49.0	-52.8	-36.7	-63.7
BCP2	0.0105	0.0418	0.0019	-0.0066	-	-8.7	-4.8	-6.7	-19.1
[2O1HTMG][NTf <sub>2</sub> ] 286_56_cis_c4									
BCP1	0.0342	0.1202	0.0004	-0.0293	74.78	-38.5	-40.2	-28.8	-52.0
BCP2	0.017	0.0619	0.0022	-0.011	17.38	-14.4	-14.5	-12.8	-28.1
BCP3	0.014	0.0486	0.0017	-0.0088	3.14	-11.6	-10.0	-10.0	-23.9
BCP4	0.0104	0.0347	0.0011	-0.0064	12.18	-8.4	-4.6	-6.6	-18.9
BCP5	0.0122	0.0466	0.0021	-0.0075	-	-9.8	-7.3	-8.3	-21.4

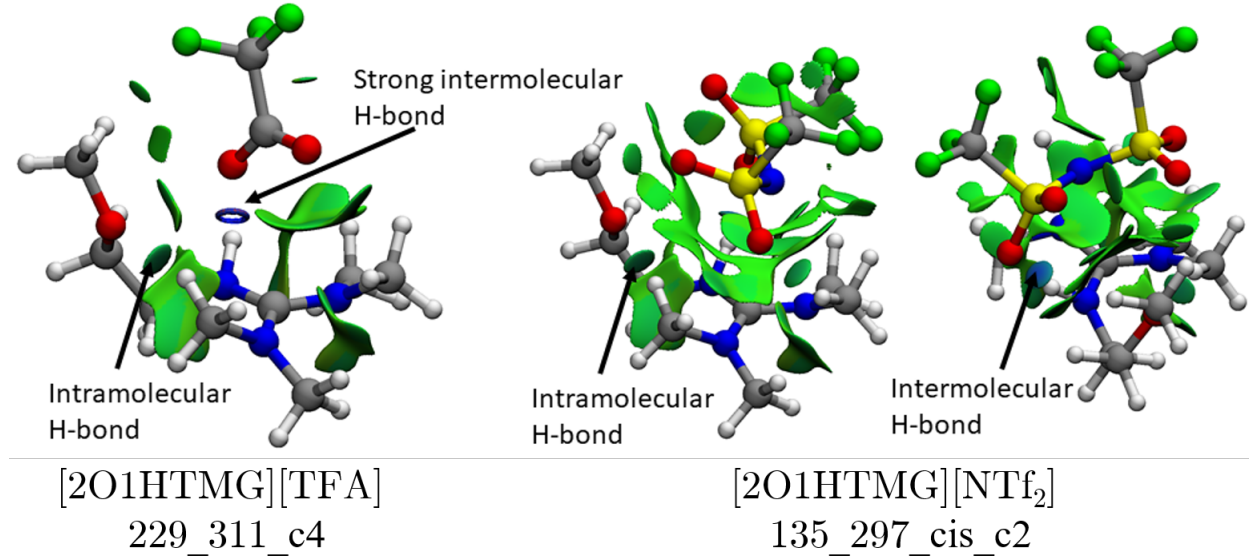


**Figure S14** NCI plots ( $\rho(x)$  cut-off: 0.05 a.u., grid spacing: 0.025 Å,  $s = 0.5$ , colored in the -0.05 to 0.05 a.u.  $\text{sign}(\lambda_2)\rho(x)$  range) for the lowest energy ion pair structures of [2O1HTMG][TFA] and [2O1HTMG][NTf<sub>2</sub>] at the B3LYP-GD3BJ/6-311+G(d,p) level of theory.

### S10.4.3 Proton Scan

A two-dimensional PES (Fig. S15) for the proton transfer from the cation to the anion in the lowest energy IP of [2O1HTMG][TFA] (229\_311\_c4) was computed by systematically changing the N-H (0.90 to 1.86 Å) and O-H (1.02 to 1.86 Å) distances in steps of 0.06 Å. The resulting structures were optimized under partial restraints (with the N-H and O-H distances being frozen) at the B3LYP-GD3BJ/6-311+G(d,p) level of theory. Single point calculations at the frozen MP2/cc-pVTZ level of theory were performed on the B3LYP optimized geometries to obtain more reliable energies.

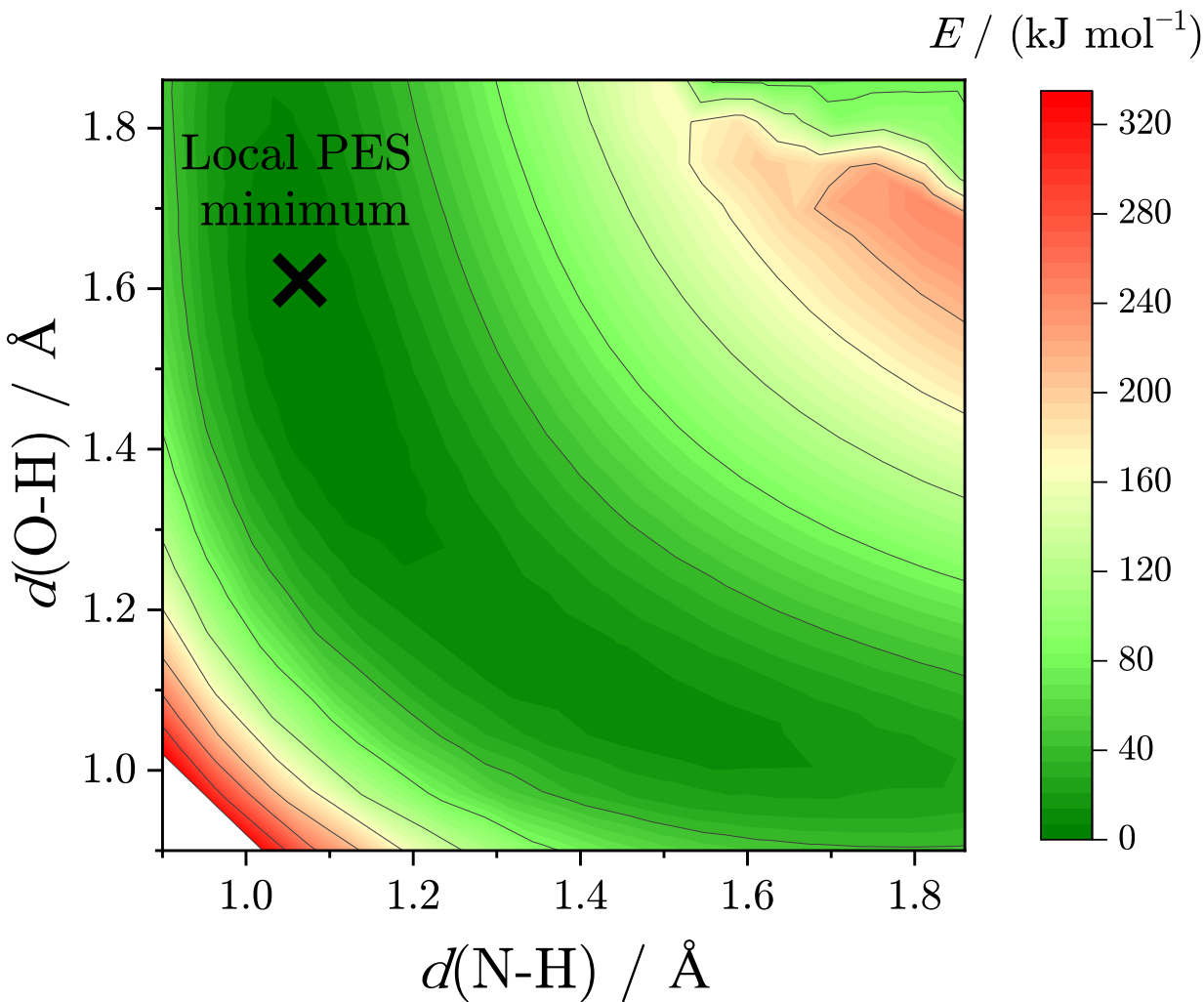


**Figure S15** Potential energy surface for the N-H bond length vs the O-H bond length in [2O1HTMG][TFA]\_229\_311\_c4. The black cross identifies the only PES minimum obtained. The level of theory is: frozen core MP2/cc-pVTZ//B3LYP-GD3BJ/6-311+G(d,p).

## S11 Two-dimensional NMR spectra

Two-dimensional NMR spectroscopy was used to gain deeper insight into the localization of the acidic proton and its exchange rate. These spectra included the three NMR-active nuclei  $^1\text{H}$ ,  $^{13}\text{C}$  and  $^{15}\text{N}$  in the cation. For this purpose,  $^1\text{H}$ - $^1\text{H}$  correlation spectroscopy (COSY),  $^1\text{H}$ - $^{13}\text{C}$  heteronuclear multiple bond correlation (HMBC) and  $^1\text{H}$ - $^{15}\text{N}$  heteronuclear single quantum coherence (HSQC) experiments were recorded. All the spectra were measured in pure substance with external referencing using coaxial NMR-tubes under the same conditions. For the ether containing ionic liquids with the  $[\text{FSI}]^-$ ,  $[\text{NTf}_2]^-$ ,  $[\text{BETI}]$ ,  $[\text{PF}_6]^-$  and  $[\text{BF}_4]^-$  anions, the situation of the acidic cation is similar. Therefore, only the spectra for [2O2HTMG][FSI] are shown here (Fig. S16 to Fig. S18). In these spectra clear correlations between the acidic proton and its vicinal protons ( $^1\text{H}$ - $^1\text{H}$  COSY) and carbons ( $^1\text{H}$ - $^{13}\text{C}$  HMBC) as well as to its carrier nitrogen atom ( $^1\text{H}$ - $^{15}\text{N}$  HSQC) revealed a strong binding to the cation and low exchange rate. In comparison, the acidic proton in [2O2HTMG][OTf] showed much weaker cross-peaks in the  $^1\text{H}$ - $^1\text{H}$  COSY (Fig. S19) and  $^1\text{H}$ - $^{15}\text{N}$  HSQC (Fig. S21) and none at all in the  $^1\text{H}$ - $^{13}\text{C}$  HMBC (Fig. S20), while for the ionic liquid with the trifluoroacetate anion, [2O2HTMG][TFA], no more cross-correlations were visible in all three spectra (Fig. S22 to Fig. S24). This indicates a rapid exchange of the acidic proton for the  $[\text{TFA}]^-$  sample, while the triflate ionic liquid occupy an intermediate position in this context (see also results discussed in the main manuscript regarding signal splitting in the one-dimensional  $^1\text{H}$ - and  $^{15}\text{N}$ -NMR spectra).

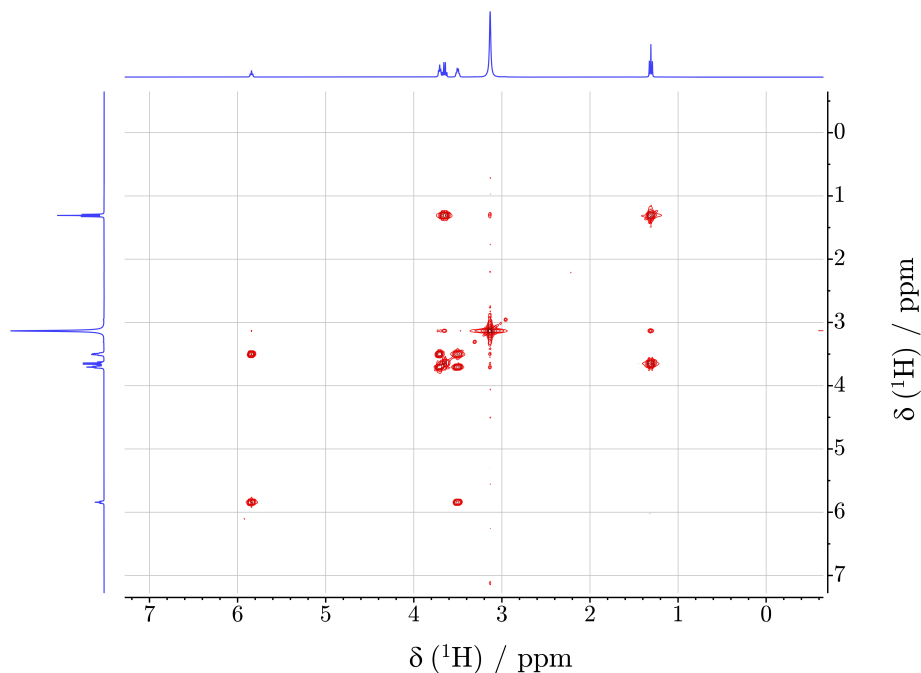
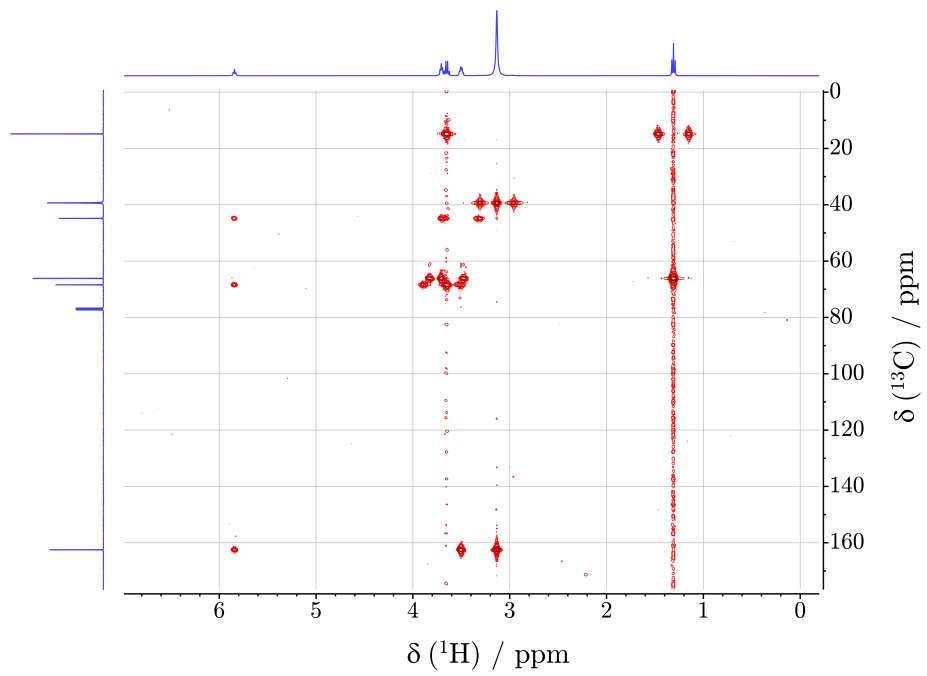
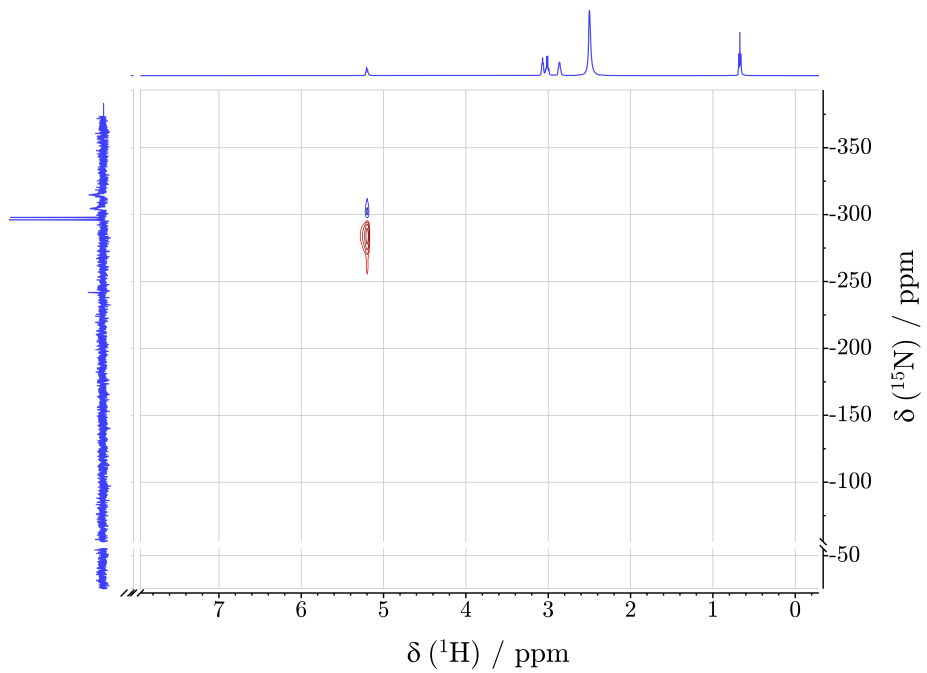


Figure S16  $^1\text{H}$ - $^1\text{H}$  correlation spectroscopy (COSY) NMR spectrum of [2O2HTMG][FSI].



**Figure S17**  $^1\text{H}$ - $^{13}\text{C}$  heteronuclear multiple bond correlation (HMBC) NMR spectrum of [2O2HTMG][FSI].



**Figure S18**  $^1\text{H}$ - $^{15}\text{N}$  heteronuclear single quantum coherence experiments (HSQC) NMR spectrum of [2O2HTMG][FSI].

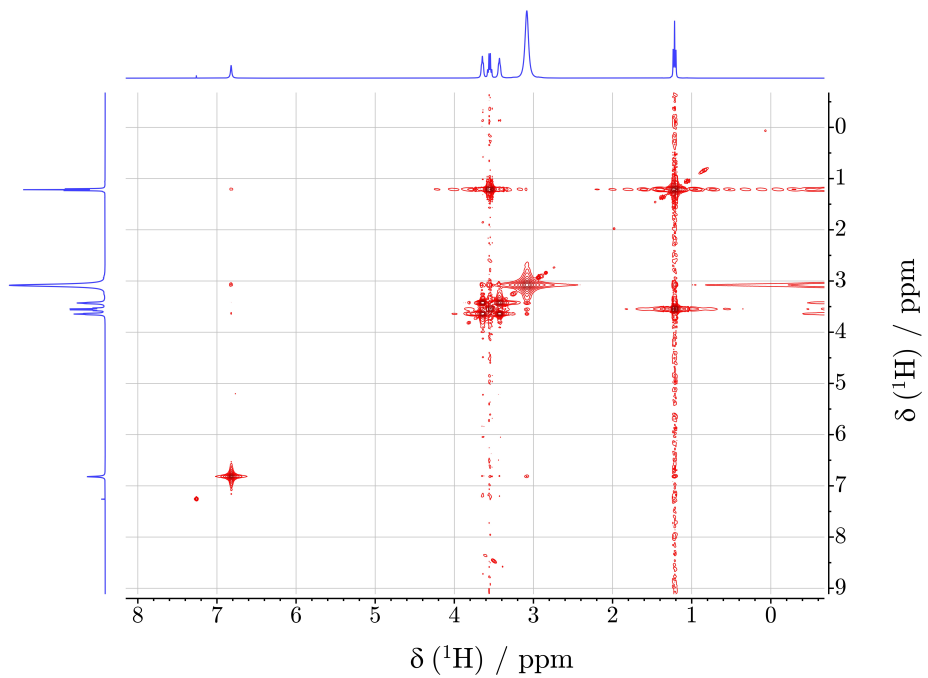


**Figure S19**  $^1\text{H}$ - $^1\text{H}$  correlation spectroscopy (COSY) NMR spectrum of [2O2HMTG][OTf].

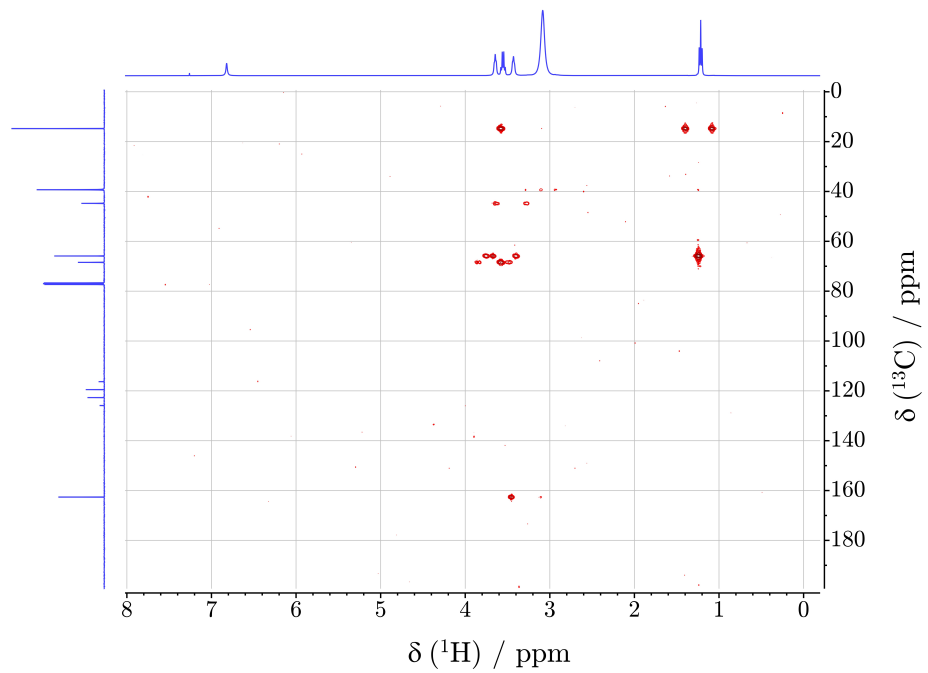


**Figure S20**  $^1\text{H}$ - $^{13}\text{C}$  heteronuclear multiple bond correlation (HMBC) NMR spectrum of [2O2HMTG][OTf].

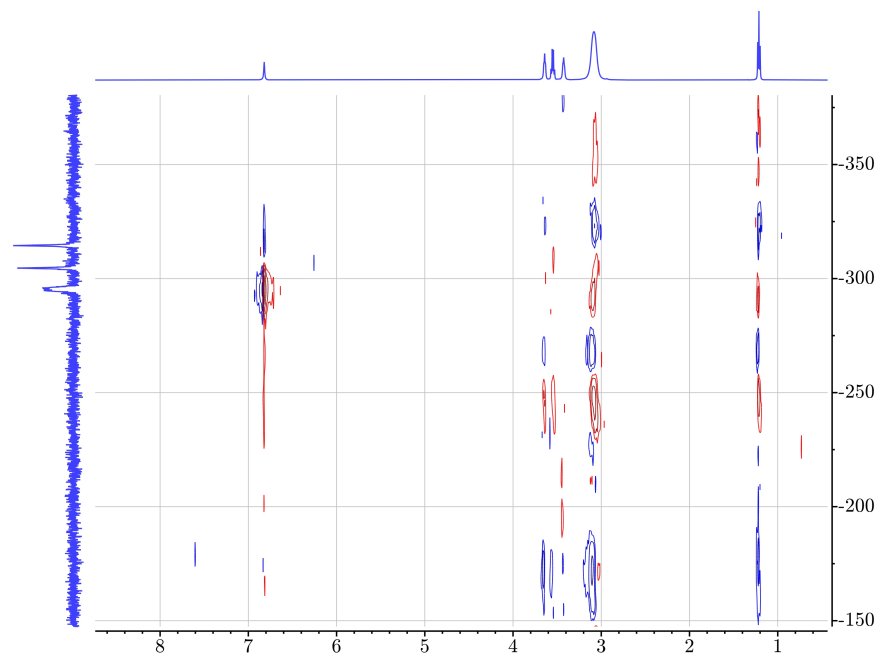


**Figure S21**  $^1\text{H}$ - $^{15}\text{N}$  heteronuclear single quantum coherence experiments (HSQC) NMR spectrum of [2O2HTMG][OTf].

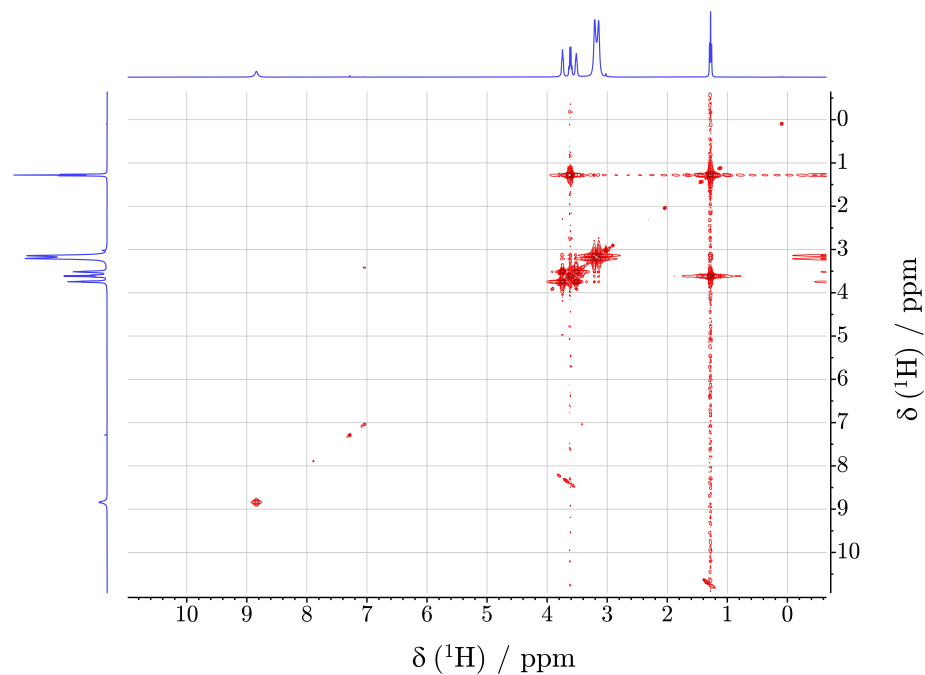


**Figure S22**  $^1\text{H}$ - $^1\text{H}$  correlation spectroscopy (COSY) NMR spectrum of [2O2HTMG][TFA].

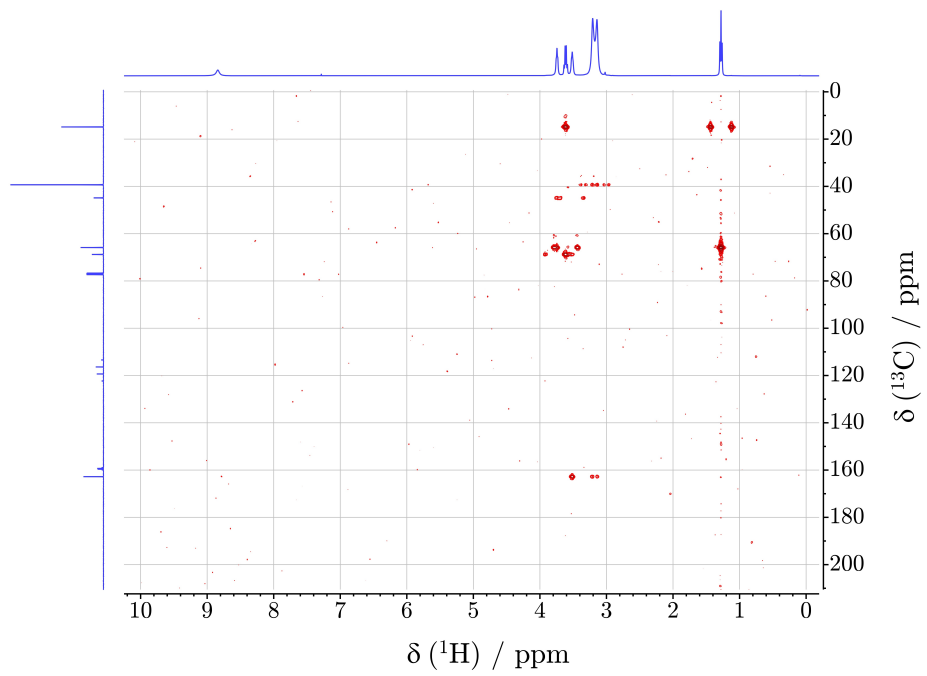


**Figure S23**  $^1\text{H}$ - $^{13}\text{C}$  heteronuclear multiple bond correlation (HMBC) NMR spectrum of [2O2HTMG][TFA].

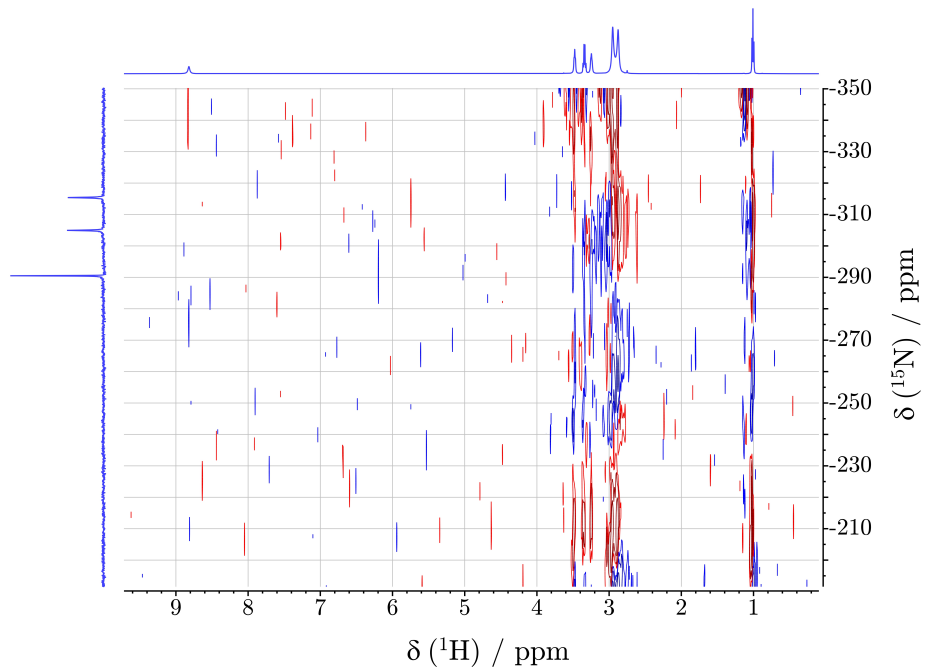


**Figure S24**  $^1\text{H}$ - $^{15}\text{N}$  heteronuclear single quantum coherence experiments (HSQC) NMR spectrum of [2O2HTMG][TFA].

## **S12 Crystal data and structure refinement**

Crystal data and structure refinement data for the single crystals of the two ionic liquids are summarized in Table S18. Further data for [C<sub>5</sub>HTMG][PF<sub>6</sub>] is given in Table S19 to Table S25, for [2O2HTMG][PF<sub>6</sub>] in Table S26 to Table S32.

**Table S18** Crystal data and structure refinement for [2O2HTMG][PF<sub>6</sub>] and [C<sub>5</sub>HTMG][PF<sub>6</sub>].

	[2O2HTMG][PF <sub>6</sub> ]	[C <sub>5</sub> HTMG][PF <sub>6</sub> ]
Empirical formula	C9 H22 F6 N3 O P	C10 H24 F6 N3 P
Formula weight	333.26 g mol <sup>-1</sup>	331.29 g mol <sup>-1</sup>
Temperature	133(2) K	152(2) K
Wavelength	0.71073 Å	0.71073 Å
Crystal system	Monoclinic	Monoclinic
Space group	P2 <sub>1</sub> /c	Cc
Unit cell dimensions	a = 8.2155(7) Å b = 15.5131(14) Å c = 12.1578(10) Å α = 90° β = 105.340(3)° γ = 90°	a = 8.4524(6) Å b = 16.1240(12) Å c = 12.1441(10) Å α = 90° β = 105.641 (4)° γ = 90°
Volume	1494.3(2) Å <sup>3</sup>	1593.8(2) Å <sup>3</sup>
Z	4	4
Density (calculated)	1.481 g cm <sup>-3</sup>	1.381 g cm <sup>-3</sup>
Absorption coefficient	0.248 mm <sup>-1</sup>	0.228 mm <sup>-1</sup>
F(000)	696	696
Crystal size	0.18 x 0.16 x 0.03 mm <sup>3</sup>	0.38 x 0.16 x 0.07 mm <sup>3</sup>
Theta range for data collection	2.177 to 26.372°	2.526 to 28.222°
Index ranges	-10 ≤ h ≤ 10 -19 ≤ k ≤ 16 -15 ≤ l ≤ 15	-11 ≤ h ≤ 10 -21 ≤ k ≤ 21 -15 ≤ l ≤ 16
Reflections collected	10697	10614
Independent reflections	3056 [R(int) = 0.0476]	3424 [R(int) = 0.0188]
Completeness to theta = 25.242°	100.0%	100.0%
Absorption correction	Semi-empirical from equivalents	Semi-empirical from equivalents
Max. and min. transmission	0.7455 and 0.6684	0.7456 and 0.7208
Refinement method	Full-matrix least-squares on F <sup>2</sup>	Full-matrix least-squares on F <sup>2</sup>
Data / restraints / parameters	3056 / 124 / 244	3424 / 136 / 237
Goodness-of-fit on F <sup>2</sup>	1.025	1.040
Final R indices [I>2sigma(I)]	R1 = 0.0406 wR2 = 0.0890	R1 = 0.0287 wR2 = 0.0672
R indices (all data)	R1 = 0.06341 wR2 = 0.1011	R1 = 0.0342 wR2 = 0.0699
Largest diff. peak and hole	0.236 and -0.333 e Å <sup>-3</sup>	0.158 and -0.204 e Å <sup>-3</sup>

**Table S19** Atomic coordinates ( $\times 10^4$ ) and equivalent isotropic displacement parameters ( $\text{\AA}^2 \times 10^3$ ) for [2O2HTMG][PF<sub>6</sub>]. U(eq) is defined as one third of the trace of the orthogonalized U<sup>ij</sup> tensor.

	x	y	z	U(eq)
P(1)	-423(1)	2876(1)	1057(1)	29(1)
F(1A)	-466(4)	3892(1)	1215(2)	59(1)
F(2A)	-315(6)	2978(3)	-198(3)	62(1)
F(3A)	1571(5)	2874(3)	1521(5)	52(1)
F(4A)	-415(5)	1858(1)	924(2)	54(1)
F(5A)	-576(4)	2762(2)	2334(2)	50(1)
F(6A)	-2445(4)	2886(3)	613(3)	51(1)
F(1B)	295(16)	3829(6)	781(12)	61(4)
F(2B)	-300(20)	2668(12)	-230(13)	57(4)
F(3B)	1460(20)	2562(11)	1507(19)	51(4)
F(4B)	-1147(17)	1987(8)	1168(12)	58(3)
F(5B)	-516(18)	3205(13)	2219(11)	68(4)
F(6B)	-2287(17)	3261(9)	507(14)	43(3)
O(1)	6622(2)	4874(1)	3976(1)	35(1)
N(1)	4274(2)	5653(1)	1702(1)	28(1)
N(2)	6946(2)	5960(1)	1510(1)	28(1)
N(3)	6147(2)	4541(1)	1624(1)	28(1)
C(1)	5796(2)	5389(1)	1629(2)	24(1)
C(2)	4069(3)	6445(1)	2302(2)	39(1)
C(3)	2765(3)	5130(2)	1315(2)	38(1)
C(4)	6497(3)	6787(1)	925(2)	35(1)
C(5)	8743(3)	5752(2)	1832(2)	37(1)
C(6)	5761(3)	3917(1)	2426(2)	32(1)
C(7)	6887(3)	4028(1)	3619(2)	34(1)
C(8)	7520(3)	5039(2)	5128(2)	45(1)
C(9)	7336(3)	5971(2)	5388(2)	49(1)

**Table S20** Bond length for [2O2HTMG][PF<sub>6</sub>].

Bond	Bond length / Å	Bond	Bond length / Å
P(1)-F(4B)	1.522(10)	C(2)-H(2A)	0.9800
P(1)-F(5B)	1.522(12)	C(2)-H(2B)	0.9800
P(1)-F(2A)	1.561(3)	C(2)-H(2C)	0.9800
P(1)-F(3B)	1.579(16)	C(3)-H(3A)	0.9800
P(1)-F(3A)	1.585(4)	C(3)-H(3B)	0.9800
P(1)-F(4A)	1.586(2)	C(3)-H(3C)	0.9800
P(1)-F(1A)	1.5893(19)	C(4)-H(4A)	0.9800
P(1)-F(5A)	1.600(3)	C(4)-H(4B)	0.9800
P(1)-F(6A)	1.605(3)	C(4)-H(4C)	0.9800
P(1)-F(6B)	1.615(13)	C(5)-H(5A)	0.9800
P(1)-F(2B)	1.628(15)	C(5)-H(5B)	0.9800
P(1)-F(1B)	1.659(8)	C(5)-H(5C)	0.9800
O(1)-C(7)	1.417(2)	C(6)-C(7)	1.510(3)
O(1)-C(8)	1.423(3)	C(6)-H(6A)	0.9900
N(1)-C(1)	1.340(2)	C(6)-H(6B)	0.9900
N(1)-C(3)	1.452(3)	C(7)-H(7A)	0.9900
N(1)-C(2)	1.462(3)	C(7)-H(7B)	0.9900
N(2)-C(1)	1.331(2)	C(8)-C(9)	1.497(3)
N(2)-C(5)	1.460(3)	C(8)-H(8A)	0.9900
N(2)-C(4)	1.466(3)	C(8)-H(8B)	0.9900
N(3)-C(1)	1.347(2)	C(9)-H(9A)	0.9800
N(3)-C(6)	1.466(3)	C(9)-H(9B)	0.9800
N(3)-H(3N)	0.873(10)	C(9)-H(9C)	0.9800

**Table S21** Bond length and angles for [2O2HTMG][PF<sub>6</sub>].

Bond	Angle / degrees	Bond	Angle / degrees
F(4B)-P(1)-F(5B)	96.1(7)	N(1)-C(2)-H(2C)	109.5
F(4B)-P(1)-F(3B)	93.5(7)	H(2A)-C(2)-H(2C)	109.5
F(5B)-P(1)-F(3B)	93.9(9)	H(2B)-C(2)-H(2C)	109.5
F(2A)-P(1)-F(3A)	91.5(2)	N(1)-C(3)-H(3A)	109.5
F(2A)-P(1)-F(4A)	89.88(16)	N(1)-C(3)-H(3B)	109.5
F(3A)-P(1)-F(4A)	90.19(15)	H(3A)-C(3)-H(3B)	109.5
F(2A)-P(1)-F(1A)	91.47(16)	N(1)-C(3)-H(3C)	109.5
F(3A)-P(1)-F(1A)	90.70(15)	H(3A)-C(3)-H(3C)	109.5
F(4A)-P(1)-F(1A)	178.36(13)	H(3B)-C(3)-H(3C)	109.5
F(2A)-P(1)-F(5A)	178.7(2)	N(2)-C(4)-H(4A)	109.5
F(3A)-P(1)-F(5A)	89.7(2)	N(2)-C(4)-H(4B)	109.5
F(4A)-P(1)-F(5A)	89.64(13)	H(4A)-C(4)-H(4B)	109.5
F(1A)-P(1)-F(5A)	89.00(12)	N(2)-C(4)-H(4C)	109.5
F(2A)-P(1)-F(6A)	89.5(2)	H(4A)-C(4)-H(4C)	109.5
F(3A)-P(1)-F(6A)	178.8(2)	H(4B)-C(4)-H(4C)	109.5
F(4A)-P(1)-F(6A)	90.45(14)	N(2)-C(5)-H(5A)	109.5
F(1A)-P(1)-F(6A)	88.63(13)	N(2)-C(5)-H(5B)	109.5
F(5A)-P(1)-F(6A)	89.27(17)	H(5A)-C(5)-H(5B)	109.5
F(4B)-P(1)-F(6B)	91.2(5)	N(2)-C(5)-H(5C)	109.5
F(5B)-P(1)-F(6B)	89.2(8)	H(5A)-C(5)-H(5C)	109.5
F(3B)-P(1)-F(6B)	174.0(9)	H(5B)-C(5)-H(5C)	109.5
F(4B)-P(1)-F(2B)	91.8(8)	N(3)-C(6)-C(7)	112.24(18)
F(5B)-P(1)-F(2B)	171.8(9)	N(3)-C(6)-H(6A)	109.2
F(3B)-P(1)-F(2B)	88.0(10)	C(7)-C(6)-H(6A)	109.2
F(6B)-P(1)-F(2B)	88.2(8)	N(3)-C(6)-H(6B)	109.2
F(4B)-P(1)-F(1B)	173.6(6)	C(7)-C(6)-H(6B)	109.2
F(5B)-P(1)-F(1B)	89.8(7)	H(6A)-C(6)-H(6B)	107.9
F(3B)-P(1)-F(1B)	88.6(7)	O(1)-C(7)-C(6)	107.16(16)
F(6B)-P(1)-F(1B)	86.3(5)	O(1)-C(7)-H(7A)	110.3
F(2B)-P(1)-F(1B)	82.2(7)	C(6)-C(7)-H(7A)	110.3
C(7)-O(1)-C(8)	112.70(16)	O(1)-C(7)-H(7B)	110.3
C(1)-N(1)-C(3)	122.61(18)	C(6)-C(7)-H(7B)	110.3
C(1)-N(1)-C(2)	121.50(18)	H(7A)-C(7)-H(7B)	108.5
C(3)-N(1)-C(2)	115.52(18)	O(1)-C(8)-C(9)	109.0(2)
C(1)-N(2)-C(5)	121.38(17)	O(1)-C(8)-H(8A)	109.9
C(1)-N(2)-C(4)	122.73(17)	C(9)-C(8)-H(8A)	109.9
C(5)-N(2)-C(4)	115.47(17)	O(1)-C(8)-H(8B)	109.9
C(1)-N(3)-C(6)	123.83(17)	C(9)-C(8)-H(8B)	109.9
C(1)-N(3)-H(3N)	115.5(15)	H(8A)-C(8)-H(8B)	108.3
C(6)-N(3)-H(3N)	113.7(15)	C(8)-C(9)-H(9A)	109.5
N(2)-C(1)-N(1)	120.34(18)	C(8)-C(9)-H(9B)	109.5
N(2)-C(1)-N(3)	119.38(18)	H(9A)-C(9)-H(9B)	109.5
N(1)-C(1)-N(3)	120.21(18)	C(8)-C(9)-H(9C)	109.5
N(1)-C(2)-H(2A)	109.5	H(9A)-C(9)-H(9C)	109.5
N(1)-C(2)-H(2B)	109.5	H(9B)-C(9)-H(9C)	109.5
H(2A)-C(2)-H(2B)	109.5		

**Table S22** Anisotropic displacement parameters ( $\text{\AA}^2 \times 10^3$ ) for [2O2HTMG][PF<sub>6</sub>]. The anisotropic displacement factor exponent takes the form:  $-2\pi^2[h^2 a^{*2}U^{11} + \dots + 2 h k a^* b^* U^{12}]$ .

	U <sup>11</sup>	U <sup>22</sup>	U <sup>33</sup>	U <sup>23</sup>	U <sup>13</sup>	U <sup>12</sup>
P(1)	31(1)	26(1)	29(1)	0(1)	8(1)	3(1)
F(1A)	61(2)	24(1)	92(2)	0(1)	21(1)	2(1)
F(2A)	71(2)	84(3)	38(2)	25(2)	30(1)	30(2)
F(3A)	32(1)	58(2)	62(2)	-3(2)	7(1)	5(1)
F(4A)	75(2)	29(1)	55(1)	-8(1)	14(1)	2(1)
F(5A)	66(1)	57(2)	31(1)	3(1)	19(1)	14(1)
F(6A)	32(1)	70(2)	50(1)	-8(2)	5(1)	0(1)
F(1B)	44(6)	33(5)	100(7)	21(5)	6(5)	-15(4)
F(2B)	43(6)	90(10)	35(6)	-33(7)	2(4)	15(7)
F(3B)	35(6)	59(9)	52(6)	14(8)	2(5)	15(6)
F(4B)	57(7)	46(6)	67(6)	27(5)	6(5)	-15(5)
F(5B)	58(6)	113(10)	29(5)	-27(7)	4(4)	14(8)
F(6B)	27(5)	53(7)	45(5)	-1(6)	4(4)	6(5)
O(1)	47(1)	28(1)	29(1)	0(1)	10(1)	4(1)
N(1)	29(1)	25(1)	32(1)	2(1)	11(1)	4(1)
N(2)	30(1)	24(1)	29(1)	0(1)	7(1)	0(1)
N(3)	34(1)	21(1)	31(1)	0(1)	14(1)	3(1)
C(1)	30(1)	24(1)	20(1)	-1(1)	5(1)	1(1)
C(2)	51(1)	31(1)	39(1)	0(1)	21(1)	12(1)
C(3)	30(1)	38(1)	45(1)	8(1)	9(1)	0(1)
C(4)	42(1)	26(1)	38(1)	6(1)	10(1)	-2(1)
C(5)	27(1)	37(1)	43(1)	-2(1)	5(1)	-4(1)
C(6)	41(1)	21(1)	37(1)	2(1)	15(1)	2(1)
C(7)	43(1)	27(1)	35(1)	4(1)	13(1)	6(1)
C(8)	56(2)	46(2)	30(1)	-2(1)	7(1)	-2(1)
C(9)	61(2)	47(2)	42(1)	-11(1)	19(1)	-11(1)

**Table S23** Hydrogen coordinates ( $\times 10^4$ ) and isotropic displacement parameters ( $\text{\AA}^2 \times 10^3$ ) for [2O2HTMG][PF<sub>6</sub>].

	x	y	z	U(eq)
H(3N)	7036(19)	4408(14)	1395(17)	34
H(2A)	3420	6864	1756	58
H(2B)	5182	6686	2673	58
H(2C)	3468	6317	2880	58
H(3A)	1842	5487	867	57
H(3B)	2449	4892	1976	57
H(3C)	2987	4657	839	57
H(4A)	7122	6858	347	53
H(4B)	6786	7258	1480	53
H(4C)	5282	6799	556	53
H(5A)	9051	5491	1181	55
H(5B)	8985	5346	2471	55
H(5C)	9400	6281	2060	55
H(6A)	5897	3326	2157	39
H(6B)	4569	3988	2440	39
H(7A)	6598	3598	4139	41
H(7B)	8084	3949	3624	41
H(8A)	8728	4895	5245	54
H(8B)	7065	4675	5647	54
H(9A)	7795	6327	4875	73
H(9B)	7954	6090	6180	73
H(9C)	6139	6107	5278	73

**Table S24** Torsion angles for [2O2HTMG][PF<sub>6</sub>].

Bond	Torsion angle / degrees
C(5)-N(2)-C(1)-N(1)	157.62(18)
C(4)-N(2)-C(1)-N(1)	-30.2(3)
C(5)-N(2)-C(1)-N(3)	-25.3(3)
C(4)-N(2)-C(1)-N(3)	146.86(19)
C(3)-N(1)-C(1)-N(2)	150.76(19)
C(2)-N(1)-C(1)-N(2)	-36.6(3)
C(3)-N(1)-C(1)-N(3)	-26.3(3)
C(2)-N(1)-C(1)-N(3)	146.39(19)
C(6)-N(3)-C(1)-N(2)	136.2(2)
C(6)-N(3)-C(1)-N(1)	-46.7(3)
C(1)-N(3)-C(6)-C(7)	-71.1(3)
C(8)-O(1)-C(7)-C(6)	175.47(18)
N(3)-C(6)-C(7)-O(1)	60.1(2)
C(7)-O(1)-C(8)-C(9)	173.24(19)

**Table S25** Hydrogen bonds for [2O2HTMG][PF<sub>6</sub>].

D-H···A	d(D-H)	d(H···A)	d(D···A)	<(DHA)
N(3)-H(3N)...F(1A <sup>a</sup> )#1	0.873(10)	2.267(11)	3.120(4)	166.0(19)
N(3)-H(3N)...F(6B <sup>b</sup> )#1	0.873(10)	2.23(2)	2.893(15)	133.0(19)

Symmetry transformations used to generate equivalent atoms: #1 x+1,y,z

**Table S26** Atomic coordinates ( $\times 10^4$ ) and equivalent isotropic displacement parameters ( $\text{\AA}^2 \times 10^3$ ) for  $[\text{C}_5\text{HTMG}][\text{PF}_6]$ . U(eq) is defined as one third of the trace of the orthogonalized  $U^{ij}$  tensor.

	x	y	z	U(eq)
P(1)	2296(1)	6572(1)	5374(1)	31(1)
F(1)	1380(2)	6022(1)	6096(1)	58(1)
F(2)	3925(2)	6525(1)	6389(1)	60(1)
F(3)	3229(2)	7115(1)	4647(1)	48(1)
F(4)	670(2)	6622(1)	4345(1)	50(1)
F(5)	2833(2)	5754(1)	4825(2)	60(1)
F(6)	1754(3)	7385(1)	5910(1)	71(1)
N(1)	3473(3)	3968(1)	4863(2)	38(1)
N(2)	2437(2)	2640(1)	4883(2)	34(1)
N(3)	2542(2)	3546(1)	6387(2)	34(1)
C(1)	2816(3)	3385(1)	5366(2)	31(1)
C(2A)	4418(8)	3807(5)	4063(5)	33(1)
C(3A)	5962(6)	4322(3)	4427(4)	34(1)
C(4A)	6994(4)	4228(2)	3584(3)	32(1)
C(5A)	8514(6)	4758(3)	3849(4)	46(1)
C(6A)	9480(11)	4687(9)	2985(8)	43(2)
C(2B)	4912(13)	3914(8)	4316(10)	32(2)
C(3B)	6470(11)	4372(5)	4942(8)	40(2)
C(4B)	7901(9)	4304(4)	4363(6)	40(2)
C(5B)	7589(9)	4729(4)	3241(7)	40(2)
C(6B)	9049(19)	4701(17)	2731(17)	49(4)
C(7)	1916(4)	2522(2)	3648(2)	55(1)
C(8)	2546(3)	1886(1)	5557(2)	40(1)
C(9)	1118(3)	3215(2)	6703(2)	45(1)
C(10)	3440(4)	4196(2)	7125(2)	45(1)

**Table S27** Bond length for  $[C_5HTMG][PF_6]$ .

Bond	Bond length / Å	Bond	Bond length / Å
P(1)-F(2)	1.5831(16)	C(6A)-H(6B)	0.9800
P(1)-F(6)	1.5852(18)	C(6A)-H(6C)	0.9800
P(1)-F(1)	1.5885(16)	C(2B)-C(3B)	1.522(12)
P(1)-F(4)	1.5904(16)	C(2B)-H(2C)	0.9900
P(1)-F(3)	1.5934(15)	C(2B)-H(2D)	0.9900
P(1)-F(5)	1.5976(16)	C(3B)-C(4B)	1.559(11)
N(1)-C(1)	1.322(3)	C(3B)-H(3C)	0.9900
N(1)-C(2A)	1.438(7)	C(3B)-H(3D)	0.9900
N(1)-C(2B)	1.538(12)	C(4B)-C(5B)	1.483(10)
N(1)-H(1N)	0.863(13)	C(4B)-H(4C)	0.9900
N(2)-C(1)	1.337(3)	C(4B)-H(4D)	0.9900
N(2)-C(8)	1.454(3)	C(5B)-C(6B)	1.52(2)
N(2)-C(7)	1.458(3)	C(5B)-H(5C)	0.9900
N(3)-C(1)	1.346(3)	C(5B)-H(5D)	0.9900
N(3)-C(10)	1.454(3)	C(6B)-H(6D)	0.9800
N(3)-C(9)	1.460(3)	C(6B)-H(6E)	0.9800
C(2A)-C(3A)	1.508(6)	C(6B)-H(6F)	0.9800
C(2A)-H(2A)	0.9900	C(7)-H(7A)	0.9800
C(2A)-H(2B)	0.9900	C(7)-H(7B)	0.9800
C(3A)-C(4A)	1.521(6)	C(7)-H(7C)	0.9800
C(3A)-H(3A)	0.9900	C(8)-H(8A)	0.9800
C(3A)-H(3B)	0.9900	C(8)-H(8B)	0.9800
C(4A)-C(5A)	1.505(5)	C(8)-H(8C)	0.9800
C(4A)-H(4A)	0.9900	C(9)-H(9A)	0.9800
C(4A)-H(4B)	0.9900	C(9)-H(9B)	0.9800
C(5A)-C(6A)	1.498(12)	C(9)-H(9C)	0.9800
C(5A)-H(5A)	0.9900	C(10)-H(10A)	0.9800
C(5A)-H(5B)	0.9900	C(10)-H(10B)	0.9800
C(6A)-H(6A)	0.9800	C(10)-H(10C)	0.9800

**Table S28** Bond length and angles for [C<sub>5</sub>HTMG][PF<sub>6</sub>].

Bond	Angle / degrees	Bond	Angle / degrees
F(2)-P(1)-F(6)	90.37(11)	H(6A)-C(6A)-H(6C)	109.5
F(2)-P(1)-F(1)	89.64(9)	H(6B)-C(6A)-H(6C)	109.5
F(6)-P(1)-F(1)	89.78(12)	C(3B)-C(2B)-N(1)	115.9(8)
F(2)-P(1)-F(4)	179.47(11)	C(3B)-C(2B)-H(2C)	108.3
F(6)-P(1)-F(4)	89.80(10)	N(1)-C(2B)-H(2C)	108.3
F(1)-P(1)-F(4)	90.87(9)	C(3B)-C(2B)-H(2D)	108.3
F(2)-P(1)-F(3)	90.11(9)	N(1)-C(2B)-H(2D)	108.3
F(6)-P(1)-F(3)	90.85(11)	H(2C)-C(2B)-H(2D)	107.4
F(1)-P(1)-F(3)	179.32(11)	C(2B)-C(3B)-C(4B)	114.4(7)
F(4)-P(1)-F(3)	89.39(8)	C(2B)-C(3B)-H(3C)	108.7
F(2)-P(1)-F(5)	90.01(11)	C(4B)-C(3B)-H(3C)	108.7
F(6)-P(1)-F(5)	179.61(11)	C(2B)-C(3B)-H(3D)	108.7
F(1)-P(1)-F(5)	90.29(11)	C(4B)-C(3B)-H(3D)	108.7
F(4)-P(1)-F(5)	89.82(10)	H(3C)-C(3B)-H(3D)	107.6
F(3)-P(1)-F(5)	89.08(9)	C(5B)-C(4B)-C(3B)	114.5(6)
C(1)-N(1)-C(2A)	124.3(4)	C(5B)-C(4B)-H(4C)	108.6
C(1)-N(1)-C(2B)	129.8(5)	C(3B)-C(4B)-H(4C)	108.6
C(1)-N(1)-H(1N)	116(2)	C(5B)-C(4B)-H(4D)	108.6
C(2A)-N(1)-H(1N)	119(2)	C(3B)-C(4B)-H(4D)	108.6
C(2B)-N(1)-H(1N)	111(2)	H(4C)-C(4B)-H(4D)	107.6
C(1)-N(2)-C(8)	122.18(19)	C(4B)-C(5B)-C(6B)	113.4(9)
C(1)-N(2)-C(7)	122.6(2)	C(4B)-C(5B)-H(5C)	108.9
C(8)-N(2)-C(7)	115.19(19)	C(6B)-C(5B)-H(5C)	108.9
C(1)-N(3)-C(10)	121.1(2)	C(4B)-C(5B)-H(5D)	108.9
C(1)-N(3)-C(9)	122.1(2)	C(6B)-C(5B)-H(5D)	108.9
C(10)-N(3)-C(9)	115.57(19)	H(5C)-C(5B)-H(5D)	107.7
N(1)-C(1)-N(2)	121.1(2)	C(5B)-C(6B)-H(6D)	109.5
N(1)-C(1)-N(3)	119.13(19)	C(5B)-C(6B)-H(6E)	109.5
N(2)-C(1)-N(3)	119.8(2)	H(6D)-C(6B)-H(6E)	109.5
N(1)-C(2A)-C(3A)	107.3(4)	C(5B)-C(6B)-H(6F)	109.5
N(1)-C(2A)-H(2A)	110.2	H(6D)-C(6B)-H(6F)	109.5
C(3A)-C(2A)-H(2A)	110.2	H(6E)-C(6B)-H(6F)	109.5
N(1)-C(2A)-H(2B)	110.2	N(2)-C(7)-H(7A)	109.5
C(3A)-C(2A)-H(2B)	110.2	N(2)-C(7)-H(7B)	109.5
H(2A)-C(2A)-H(2B)	108.5	H(7A)-C(7)-H(7B)	109.5
C(2A)-C(3A)-C(4A)	110.9(4)	N(2)-C(7)-H(7C)	109.5
C(2A)-C(3A)-H(3A)	109.5	H(7A)-C(7)-H(7C)	109.5
C(4A)-C(3A)-H(3A)	109.5	H(7B)-C(7)-H(7C)	109.5
C(2A)-C(3A)-H(3B)	109.5	N(2)-C(8)-H(8A)	109.5
C(4A)-C(3A)-H(3B)	109.5	N(2)-C(8)-H(8B)	109.5
H(3A)-C(3A)-H(3B)	108.1	H(8A)-C(8)-H(8B)	109.5
C(5A)-C(4A)-C(3A)	114.3(3)	N(2)-C(8)-H(8C)	109.5
C(5A)-C(4A)-H(4A)	108.7	H(8A)-C(8)-H(8C)	109.5
C(3A)-C(4A)-H(4A)	108.7	H(8B)-C(8)-H(8C)	109.5
C(5A)-C(4A)-H(4B)	108.7	N(3)-C(9)-H(9A)	109.5
C(3A)-C(4A)-H(4B)	108.7	N(3)-C(9)-H(9B)	109.5
H(4A)-C(4A)-H(4B)	107.6	H(9A)-C(9)-H(9B)	109.5
C(6A)-C(5A)-C(4A)	113.7(5)	N(3)-C(9)-H(9C)	109.5
C(6A)-C(5A)-H(5A)	108.8	H(9A)-C(9)-H(9C)	109.5
C(4A)-C(5A)-H(5A)	108.8	H(9B)-C(9)-H(9C)	109.5
C(6A)-C(5A)-H(5B)	108.8	N(3)-C(10)-H(10A)	109.5
C(4A)-C(5A)-H(5B)	108.8	N(3)-C(10)-H(10B)	109.5
H(5A)-C(5A)-H(5B)	107.7	H(10A)-C(10)-H(10B)	109.5
C(5A)-C(6A)-H(6A)	109.5	N(3)-C(10)-H(10C)	109.5
C(5A)-C(6A)-H(6B)	109.5	H(10A)-C(10)-H(10C)	109.5
H(6A)-C(6A)-H(6B)	109.5	H(10B)-C(10)-H(10C)	109.5
C(5A)-C(6A)-H(6C)	109.5		

**Table S29** Anisotropic displacement parameters ( $\text{\AA}^2 \times 10^3$ ) for  $[\text{C}_5\text{HTMG}][\text{PF}_6]$ . The anisotropic displacement factor exponent takes the form:  $-2\pi^2[h^2 a^{*2}U^{11} + \dots + 2 h k a^* b^* U^{12}]$ .

	U <sup>11</sup>	U <sup>22</sup>	U <sup>33</sup>	U <sup>23</sup>	U <sup>13</sup>	U <sup>12</sup>
P(1)	34(1)	30(1)	29(1)	2(1)	12(1)	0(1)
F(1)	49(1)	73(1)	59(1)	25(1)	27(1)	-3(1)
F(2)	44(1)	90(1)	41(1)	25(1)	2(1)	-6(1)
F(3)	50(1)	51(1)	43(1)	14(1)	12(1)	-14(1)
F(4)	40(1)	68(1)	40(1)	3(1)	7(1)	-2(1)
F(5)	87(1)	36(1)	70(1)	1(1)	40(1)	15(1)
F(6)	114(2)	55(1)	44(1)	-11(1)	22(1)	25(1)
N(1)	56(1)	25(1)	36(1)	1(1)	19(1)	5(1)
N(2)	40(1)	29(1)	31(1)	-4(1)	7(1)	3(1)
N(3)	40(1)	32(1)	31(1)	-6(1)	14(1)	-6(1)
C(1)	34(1)	29(1)	28(1)	0(1)	6(1)	5(1)
C(2A)	45(3)	27(2)	28(3)	-1(2)	13(2)	-7(2)
C(3A)	41(2)	30(2)	32(2)	-3(2)	12(2)	-5(2)
C(4A)	35(2)	27(2)	34(2)	-2(1)	10(2)	-4(1)
C(5A)	46(2)	50(2)	45(2)	-12(2)	17(2)	-15(2)
C(6A)	35(4)	52(3)	46(4)	-8(3)	14(3)	-8(3)
C(2B)	47(6)	23(4)	26(4)	-4(3)	11(4)	-1(4)
C(3B)	45(4)	45(3)	29(4)	3(3)	11(3)	-12(3)
C(4B)	35(3)	39(3)	45(4)	1(3)	9(3)	-4(3)
C(5B)	42(4)	34(3)	43(4)	0(3)	9(3)	-1(3)
C(6B)	31(7)	64(6)	51(8)	1(6)	10(5)	-6(6)
C(7)	75(2)	45(1)	36(1)	-12(1)	1(1)	8(1)
C(8)	42(1)	28(1)	54(2)	-1(1)	21(1)	1(1)
C(9)	47(1)	44(1)	52(2)	-9(1)	25(1)	-6(1)
C(10)	62(2)	40(1)	32(1)	-10(1)	14(1)	-13(1)

**Table S30** Hydrogen coordinates ( $\times 10^4$ ) and isotropic displacement parameters ( $\text{\AA}^2 \times 10^3$ ) for  $[\text{C}_5\text{HTMG}] [\text{PF}_6]$ .

	x	y	z	U(eq)
H(1N)	3300(40)	4473(10)	5030(20)	48(8)
H(2A)	3781	3962	3280	39
H(2B)	4697	3211	4068	39
H(3A)	6612	4144	5196	40
H(3B)	5666	4912	4473	40
H(4A)	7323	3639	3571	38
H(4B)	6306	4370	2809	38
H(5A)	8192	5344	3895	55
H(5B)	9228	4598	4608	55
H(6A)	9837	4111	2952	65
H(6B)	10444	5050	3205	65
H(6C)	8789	4853	2232	65
H(2C)	5188	3322	4258	38
H(2D)	4539	4137	3529	38
H(3C)	6852	4149	5729	48
H(3D)	6202	4965	5000	48
H(4C)	8906	4542	4885	48
H(4D)	8116	3710	4255	48
H(5C)	7305	5316	3335	48
H(5D)	6631	4467	2699	48
H(6D)	9275	4125	2568	73
H(6E)	10016	4938	3276	73
H(6F)	8795	5023	2020	73
H(7A)	1768	3064	3267	82
H(7B)	874	2218	3438	82
H(7C)	2754	2206	3406	82
H(8A)	3082	2010	6362	60
H(8B)	3190	1471	5278	60
H(8C)	1439	1671	5487	60
H(9A)	416	2912	6053	68
H(9B)	494	3672	6914	68
H(9C)	1487	2838	7355	68
H(10A)	4531	4258	7000	67
H(10B)	3555	4050	7926	67
H(10C)	2838	4721	6948	67

**Table S31** Torsion angles for  $[C_5HTMG][PF_6]$ .

Bond	Torsion angle / degrees
C(2A)-N(1)-C(1)-N(2)	-25.6(4)
C(2B)-N(1)-C(1)-N(2)	-47.3(6)
C(2A)-N(1)-C(1)-N(3)	153.8(4)
C(2B)-N(1)-C(1)-N(3)	132.1(6)
C(8)-N(2)-C(1)-N(1)	147.1(2)
C(7)-N(2)-C(1)-N(1)	-31.7(4)
C(8)-N(2)-C(1)-N(3)	-32.3(3)
C(7)-N(2)-C(1)-N(3)	148.9(3)
C(10)-N(3)-C(1)-N(1)	-22.0(3)
C(9)-N(3)-C(1)-N(1)	144.4(2)
C(10)-N(3)-C(1)-N(2)	157.3(2)
C(9)-N(3)-C(1)-N(2)	-36.2(3)
C(1)-N(1)-C(2A)-C(3A)	-131.8(4)
N(1)-C(2A)-C(3A)-C(4A)	-176.7(4)
C(2A)-C(3A)-C(4A)-C(5A)	176.8(5)
C(3A)-C(4A)-C(5A)-C(6A)	-177.5(6)
C(1)-N(1)-C(2B)-C(3B)	-111.1(8)
N(1)-C(2B)-C(3B)-C(4B)	-179.9(8)
C(2B)-C(3B)-C(4B)-C(5B)	67.1(10)
C(3B)-C(4B)-C(5B)-C(6B)	176.3(12)

**Table S32** Hydrogen bonds for  $[C_5HTMG][PF_6]$ .

D-H $\cdots$ A	d(D-H)	d(H $\cdots$ A)	d(D $\cdots$ A)	$\angle$ (DHA)
N(1)-H(1N) $\cdots$ F(5)	0.863(13)	2.106(16)	2.929(2)	159(3)

## S13 References

- [1] D. Rauber, F. Philippi, J. Zapp, G. Kickelbick, H. Natter and R. Hempelmann, *RSC Advances*, 2018, **8**, 41639–41650.
- [2] K. M. Meek and Y. A. Elabd, *Macromolecules*, 2015, **48**, 7071–7084.
- [3] S. Li, Y. Lin, J. Cao and S. Zhang, *The Journal of Organic Chemistry*, 2007, **72**, 4067–4072.
- [4] C. Schreiner, S. Zugmann, R. Hartl and H. J. Gores, *Journal of Chemical & Engineering Data*, 2010, **55**, 1784–1788.
- [5] C. Schreiner, S. Zugmann, R. Hartl and H. J. Gores, *Journal of Chemical & Engineering Data*, 2010, **55**, 4372–4377.
- [6] J. C. Araque, J. J. Hettige and C. J. Margulis, *The Journal of Physical Chemistry B*, 2015, **119**, 12727–12740.
- [7] T. Lu and F. Chen, *Journal of Computational Chemistry*, 2012, **33**, 580–592.
- [8] T. Lu and F. Chen, *Journal of Molecular Graphics and Modelling*, 2012, **38**, 314–323.
- [9] F. Philippi, A. Quinten, D. Rauber, M. Springborg and R. Hempelmann, *Journal of Physical Chemistry A*, 2019, **123**, 4188–4200.
- [10] P. A. Hunt, C. R. Ashworth and R. P. Matthews, *Chemical Society Reviews*, 2015, **44**, 1257–1288.
- [11] E. Espinosa, E. Molins and C. Lecomte, *Chemical Physics Letters*, 1998, **285**, 170–173.
- [12] S. Emamian, T. Lu, H. Kruse and H. Emamian, *Journal of Computational Chemistry*, 2019, **40**, 2868–2881.